

The Spa2-related protein, Sph1p, is important for polarized growth in yeast

Terry Roemer, Laura Vallier, Yi-Jun Sheu and Michael Snyder*

Department of Biology, PO Box 208103, Yale University, New Haven, CT 06520-8103, USA

*Author for correspondence (e-mail: michael.snyder@yale.edu)

Accepted 24 November 1997; published on WWW 27 January 1998

SUMMARY

The *Saccharomyces cerevisiae* protein Sph1p is both structurally and functionally related to the polarity protein, Spa2p. Sph1p and Spa2p are predicted to share three 100-amino acid domains each exceeding 30% sequence identity, and the amino-terminal domain of each protein contains a direct repeat common to *Homo sapiens* and *Caenorhabditis elegans* protein sequences. *sph1-* and *spa2-*deleted cells possess defects in mating projection morphology and pseudohyphal growth. *sph1Δ spa2Δ* double mutants also exhibit a strong haploid invasive growth defect and an exacerbated mating projection defect relative to either *sph1Δ* or *spa2Δ* single mutants. Consistent with a role in polarized growth, Sph1p localizes to growth sites in a cell cycle-dependent manner: Sph1p concentrates as a cortical patch at the presumptive bud site in unbudded cells, at the tip of small, medium and large buds, and at the bud neck prior to cytokinesis. In pheromone-treated cells, Sph1p localizes to the tip of the mating projection. Proper localization of Sph1p to sites of active growth during budding and mating requires Spa2p. Sph1p interacts in the

two-hybrid system with three mitogen-activated protein (MAP) kinase kinases (MAPKKs): Mkk1p and Mkk2p, which function in the cell wall integrity/cell polarization MAP kinase pathway, and Ste7p, which operates in the pheromone and pseudohyphal signaling response pathways. Sph1p also interacts weakly with *STE11*, the MAPKKK known to activate *STE7*. Moreover, two-hybrid interactions between *SPH1* and *STE7* and *STE11* occur independently of *STE5*, a proposed scaffolding protein which interacts with several members of this MAP kinase module. We speculate that Spa2p and Sph1p may function during pseudohyphal and haploid invasive growth to help tether this MAP kinase module to sites of polarized growth. Our results indicate that Spa2p and Sph1p comprise two related proteins important for the control of cell morphogenesis in yeast.

Key words: Yeast, Bud site selection, Cell polarity, Pseudohyphal growth, MAP kinase module

INTRODUCTION

Polarized growth is fundamental for cell morphogenesis, cellular differentiation, and development in most organisms. The budding yeast, *Saccharomyces cerevisiae*, undergoes polarized cell growth throughout its life cycle (Lew and Reed, 1995; Pringle et al., 1995; Drubin and Nelson, 1996; Roemer et al., 1996b). During vegetative growth, yeast cells require polarized growth to initiate bud formation. Cell growth is concentrated at the tip of the bud during S phase and subsequently is distributed throughout the bud during G₂ and mitosis. In preparation for cytokinesis, polarized membrane and cell wall deposition reorients toward the mother-bud neck to aid in cell separation. Mating yeast cells also polarize their growth and form extended mating projections facilitating conjugation with partner cells (Sprague and Thorner, 1992). Analogous to multicellular organisms, polarized growth in yeast is responsive to both intrinsic and extrinsic signals and many of the molecules required for polarization are conserved.

In response to nitrogen starvation, yeast cells adopt a hyperpolarized mode of growth and undergo a dimorphic transition from a unicellular yeast form to a multicellular

pseudohyphal form (Gimeno et al., 1992; Roberts and Fink, 1994). This specific developmental cell type is exclusive to diploid *MATa/MATα* cells and can be distinguished from the yeast cell type by several criteria including cell shape, budding pattern, invasive growth properties, and cell cycle differences (Gimeno et al., 1992; Kron et al., 1994). Pseudohyphal cells are strikingly elongated compared to ellipsoidal-shaped yeast cells. Unlike yeast cells, they also fail to separate from one another, and bud preferentially from the pole opposite their birth scar. This unipolar budding pattern is believed to be different from the bipolar budding program of the yeast form, which buds from both poles of the cell (Freifelder, 1960; Chant and Pringle, 1995). The pseudohyphal form also exhibits vigorous invasive growth into the agar of plates limited for nitrogen, unlike the diploid yeast form growing on nutrient-rich plates. The cell cycle of pseudohyphal cells is also unique, possessing an extended G₂ phase and a much shorter G₁ phase than the yeast form (Kron et al., 1994). Collectively, these pseudohyphal characteristics enable the cells to form complex filamentous structures, which presumably aid the organism in foraging for nutrients. Haploid invasive growth, a genetically distinct process from pseudohyphal differentiation, is a related

response in which starved haploid cells form short filaments and grow invasively into solid media upon nutritional stress (Roberts and Fink, 1994). Unlike pseudohyphal growth, haploid invasive growth occurs independently of budding pattern or filament formation (Roberts and Fink, 1994).

Genes involved in pseudohyphal growth can be placed into two basic groups. The first group is also required for haploid invasive growth, and encompasses signal transduction components including several elements of the pheromone-responsive MAP kinase (MAPK) cascade, namely the PAK-homolog *STE20*, and *STE11* and *STE7*, which encode MAPKK kinase and MAPK kinases, respectively (Liu et al., 1993; Roberts and Fink, 1994). Analogous to the ERK MAP kinase pathway in mouse neuronal PC12 cells (Traverse et al., 1992), this yeast MAP kinase module can be activated by different input stimuli to generate distinctly different output responses (Roberts and Fink, 1994). Neither *FUS3* or *KSSI*, which encode two MAP kinases of this pathway, nor *STE5*, encoding a putative scaffolding protein for this kinase module, are required for pseudohyphal or haploid invasive growth. It is not known how the Ste11p-Ste7p module forms independently of Ste5p during pseudohyphal or haploid invasive growth, nor is it known whether a novel MAP kinase functions in this pathway.

Additional signal transduction components involved in pseudohyphal growth include the GTP-binding proteins Ras2p and Cdc42p which activate this pseudohyphal MAP kinase cascade (Mosch et al., 1996). Ste12p, the transcription factor at the base of the mating pathway, and a second transcription factor, Tec1p, synergistically activate downstream target genes involved in both pseudohyphal and haploid invasive growth (Gavriasis et al., 1996; Madhani and Fink, 1997; Mosch and Fink, 1997). Other proteins including transcription factors such as Phd1p (Gimeno and Fink, 1994) and Flo8p (Liu et al., 1996), as well as the protein kinase *ELM1* (Blacketer et al., 1993), and protein phosphatase *PPS1* (Blacketer et al., 1994), also function in the switch to pseudohyphal growth.

A second set of genes that function in pseudohyphal growth are bud site selection and polarity genes. A dominant gain-of-function allele of *RSR1/BUD1*, a general bud site selection gene required for proper budding pattern in both haploid and diploid cells (Bender and Pringle, 1989; Chant and Herskowitz, 1991), disrupts pseudohyphal formation when expressed in diploid cells (Gimeno et al., 1992). In addition, mutations in *ACT1* and *TPM1*, encoding yeast actin and tropomyosin, respectively, disrupt both the diploid budding pattern and differentiation to the pseudohyphal form, indicating that the actin cytoskeleton plays an important role in this differentiation process (Mosch and Fink, 1997; Yang et al., 1997).

The *SPA2* gene participates in the processes of bud site selection and morphogenesis during vegetative growth and mating. *SPA2* participates in the bipolar budding pattern of diploid cells; *spa2Δ/spa2Δ* cells form new buds in a progressively random pattern as the cells complete multiple cell cycles (Snyder, 1989; Zahner et al., 1996). Although haploid and homozygous diploid *spa2Δ* cells lack an obvious growth defect, *spa2Δ/spa2Δ* cells are noticeably rounder than wild-type cells (Snyder, 1989). *spa2Δ* mutants also fail to properly polarize their growth in response to mating pheromone and form either round, oval, or 'peanut-shaped' cells instead of normal 'pear-shaped' projections (Gehring and

Snyder, 1990; Chenevert et al., 1994; Yorihuri and Ohsumi, 1994; Valtz and Herskowitz, 1996). Synthetic-lethal interactions between *SPA2* and genes of the cell integrity MAP kinase cascade (Costigan et al., 1992, 1994) as well as the septin, *CDC10* (Flescher et al., 1993) provide additional evidence suggesting *SPA2* functions in the processes of polarized growth and cytokinesis.

Protein localization studies further suggest that Spa2p participates in yeast morphogenesis. Spa2p localizes to sites of polarized growth in budding yeast cells, first as a crescent-shaped patch marking the future bud site, and later to the tip of small, medium, and many large buds (Snyder, 1989; Snyder et al., 1991). Prior to cytokinesis, Spa2p accumulates at the bud neck (Snyder, 1989; Snyder et al., 1991). Spa2p also localizes to the tip of mating projections (Snyder, 1989; Gehring and Snyder, 1990). Pea2p, a protein lacking structural similarity to Spa2p, likely functions in concert with Spa2p as: (i) both proteins share identical immunolocalization profiles, (ii) localization of Spa2p and Pea2p are interdependent during both budding and mating, (iii) mutations in either gene result in genetically indistinguishable phenotypes, and (iv) both proteins have been co-immunoprecipitated (Valtz and Herskowitz, 1996; Y.-J. Sheu et al., unpublished observations).

Here we report the characterization of *SPH1*, which encodes a protein related to Spa2p. Genetic analysis reveals both *SPA2* and *SPH1* are required for pseudohyphal growth and together are needed for haploid invasive growth. Indirect immunofluorescence studies demonstrate that Sph1p localizes to sites of polarized growth throughout the budding cycle and during mating projection formation, and that proper Sph1p localization requires *SPA2*. Two-hybrid interactions between Sph1p and several MAP kinase signaling components parallel those between Spa2p and these same kinases (Y.-J. Sheu et al., unpublished observations). As this study was in the final stages, an insertional mutagenesis screen by Mosch and Fink (1997) also reported that Spa2p is important for some aspects of pseudohyphal growth, although they did not observe a requirement for haploid invasive growth. In addition, as we were preparing to submit this manuscript Arkowitz and Lowe (1997) reported a brief description of *SPH1* although very little of their characterization overlaps with ours (see Discussion). Our study shows that Spa2p and Sph1p comprise a set of proteins important for the control of many aspects of cell morphogenesis in yeast.

MATERIALS AND METHODS

Yeast strains and standard methods

Yeast strains used in this study are in the S288C background unless otherwise noted and are listed in Table 1. Genetic methods and growth media protocols were followed according to Guthrie and Fink (1991). Pseudohyphal growth was scored on synthetic low ammonia plus 2% dextrose (SLAD) medium as described by Gimeno and Fink (1994). General cloning procedures were performed as described by Sambrook et al. (1989).

PCR sequencing of *SPH1* polymorphs

A yeast cDNA library derived from a S288C strain background (Liu et al., 1993) and genomic DNA prepared from S288C (Y604), SK1 (S2065), W303 (Y542), and Σ 1278b (Y824) strain backgrounds were

used in polymerase chain reactions (PCR) using AmpliTaq DNA polymerase (Perkin Elmer) and oligonucleotides, 5'-TGGAG CTCCA GGATT ATCAG GCATC ACCTC-3' and 5'-TGGGT ACCCT TCCCA AGCTT TGTGG AATC-3' to generate a 570 nucleotide product encompassing the predicted frame shift region. Automated fluorescent DNA sequencing of these PCR products was performed by the Keck Biotechnology Resource Laboratory at the Yale School of Medicine.

Disruption of *SPH1* and *SPA2*

Deletion of *SPH1* was performed by substituting over 99% of the *SPH1* ORF (codons 5 through 658) with DNA fragments of the *HIS3* or *LEU2* gene. A *sph1Δ1::HIS3* null allele was generated in Y270 by the PCR gene disruption method of Baudin et al. (1993) using oligonucleotides 5'-CAGTA AAGTA AAAGA ATATC ATAAT GTGGC CATAA CGAAA TAAAA AGAAT GATTA GCTCA GAGCG CGCCT CGTTC AGAAT G-3' and 5'-CTGTA AATAG TGATC GAAAT AAAAT AAGAT AATAA CTAAA GAATA TATAT GACTT TACTG TACAC TCTTG GCCTC CTCTA GTA-3' and pRS303 to amplify the *HIS3* gene. (Underlined portions of primers correspond to sequences from the *HIS3* region of pRS303.) This PCR product contains the entire *HIS3* gene and is flanked at each end by approximately 60 base pairs of *SPH1* 5' or 3' untranslated sequence. Substitution of the *SPH1* locus with this DNA fragment deletes the entire *SPH1* ORF excluding the first four and last three codons. This DNA fragment was transformed into yeast strain Y270 and its substitution into the *SPH1* locus verified by PCR analysis. The resulting *sph1Δ1::HIS3* /*SPH1* strain was sporulated for tetrad analysis. The *sph1Δ1::HIS3* DNA fragment was also transformed into the yeast strains SEY6210 and SEY6211 and its substitution into the *SPH1* locus verified by PCR analysis. *Sph1* null strains in both mating types were crossed to make the homozygous *sph1Δ* strain, Y1215. Null alleles of *SPH1* and *SPA2* were similarly generated in *MATa* and *MATα* Σ 1278b strains (Y825 and Y826, respectively) by PCR using the *SPH1* oligonucleotides 5'-CAGTA AAGTA AAAGA ATATC ATAAT GTGGC CATAA CGAAA TAAAA AGAAT GATTA GCTCA GAGCG GTTTC GGTGA TGACG GTG-3' and 5'-CTGTA AATAG TGATC GAAAT AAAAT AAGAT AATAA CTAAA GAATA TATAT GACTT TACTG TACTT AGGGT GATGG TTCAC GTAGT GGGC-3' or *SPA2* oligonucleotides 5'-CATGG GTACG TCAAG CGAG TTTCT CTCGC ACATC ATAGA GATAT CTTCC ATTAC TACGT CGCGC GTTTC GGTGA TGACG GTG-3' and 5'-CGAAT TCAAA TAATT TATTT CGTCC TTCAA ACTTG CCTCT TCTAC AGTTT TTACC AGCTC CTTAG GGTGA TGGTT CACGT AGTGG GC-3' and pRS305 as template DNA. (Underlined portions of each primer correspond to common sequence which flank each of the selectable markers within the pRS303-pRS316 series of plasmids; Sikorski and Hieter, 1989). The resulting PCR products contain the entire *LEU2* gene flanked either by the *SPH1* sequences described above, or *SPA2* sequences that delete the entire *SPA2* gene except for its first 20 and last 25 codons. Disruption of *SPH1* and *SPA2* loci was verified by PCR. Diploid strains homozygous for *sph1Δ2::LEU2* and *spa2Δ4::LEU2* were constructed from appropriate crosses. To generate a diploid homozygous for both *sph1Δ* and *spa2Δ* in the Σ 1278b background, a *spa2Δ3::URA3* disruption plasmid (p210) (Gehring and Snyder, 1990) was digested with *Sall* and *HindIII* and transformed into haploid *sph1Δ2::LEU2* strains of both mating types. Haploid *sph1Δ2::LEU2 spa2Δ3::URA3* double mutants were verified by PCR and subsequently streaked out on 5-fluoro-orotic acid (5-FOA). The resulting *MATa* and *MATα sph1Δ2::LEU2 spa2Δ4::ura3* strains were then transformed with pIL30, mated, and zygotes selected. The resulting diploid *sph1Δ/sph1 spa2Δ/spa2Δ* strain (Y1177) was verified by two criteria: (i) a random budding pattern as judged by Calcofluor staining which is diagnostic of diploid *spa2Δ/spa2Δ* cells (Snyder, 1989; Zahner et al., 1996), and (ii) the inability to mate efficiently with tester strains.

Plasmids

The *SPH1* gene from Y270 was amplified by PCR using primer A (5'-CGCGGATCCCCGGAGGTATGATTAGCTCAGAATTAACGAATG-3'; the *Bam*HI site is italicized) and primer B (5'-CGCGGATCCACTTTACTGTACAGATCTATAATTG-3'; the *Bam*HI site is italicized and the *SPH1* initiation codon is underlined) and cloned into the *Bam*HI site of YCpIF17 (Foreman and Davis, 1994). The resulting plasmid, YCpIF17-*SPH1* contains a *GAL1* promoter, a translation initiation codon followed by a single hemagglutinin (HA) epitope and a 16 amino acid spacer upstream of the entire *SPH1* ORF.

SPH1-containing plasmids for two-hybrid analysis were constructed by amplifying *SPH1* from Y270 genomic DNA using primers A and B and cloning the *Bam*HI-digested PCR products into a *lexA* DNA binding domain (DBD) plasmid (pSH2.1; *HIS3*), a *GAL4* DNA binding domain plasmid (pAS1-CYH2; *TRP1*), and a *GAL4* activation domain (AD) plasmid (pACTII; *LEU2*). Additional two-hybrid plasmids used in this study are pSte7-AD (pSL2168) (Printen and Sprague, 1994), pSte7-DBD (Lex-Ste7) (Choi et al., 1994), pSte11-DBD (Lex-Ste11) (Choi et al., 1994), pSte11-AD (pSL2091) (Printen and Sprague, 1994), pSte20-DBD (pDH37) (Leberer et al., 1997), pSte20-DBD (pRL27) (Leberer et al., 1997), pFus3-DBD (Lex-Fus3) (Choi et al., 1994), and pSlit2-AD (Costigan et al., 1994). pBud6-DBD, pPea2-AD, pSpa2-DBD, pSpa2-AD, pMkk1-AD, pMkk2-AD and pPbs2-AD contain full length PCR-derived *BUD6*, *PEA2*, *SPA2*, *MKK1*, *MKK2*, or *PBS2* fragments cloned into pACTII or pSH2.1 as described by Y.-J. Sheu et al. (unpublished observations). Additional *BUD6* plasmids used in this study are pBud6(275-788)-AD (p831) and pBud6(478-788).AD (p688) (Evangelista et al., 1997) and pBud6(358-768) (Y.-J. Sheu et al., unpublished observations).

Immunoblot analysis

Protein extracts were prepared from Y270, Y602, and Y604 cells containing either YCpIF17-*SPH1* or YCpIF17 grown under selective conditions to mid-log phase. Cells were washed and lysed using glass beads in 250 μ l of 10 mM Tris-HCl (pH 7.5) containing the protease inhibitors phenylmethanesulfonyl fluoride (1 mM), pepstatin (10 μ g/ml), leupeptin (10 μ g/ml) and chemostatin (20 μ g/ml). Lysates were suspended in 500 μ l 2 \times Laemmli sample buffer (Laemmli, 1970), boiled 5 minutes and then centrifuged briefly at 1,000 *g* before separating the proteins by SDS-polyacrylamide gel electrophoresis using an 8% acrylamide minigel. The protein gel was electroblotted onto Immobilon-P (Millipore) and probed with mouse monoclonal anti-HA antibodies, 16B12 (BABC0) which were detected using goat anti-mouse horseradish peroxidase and ECL detection reagents (Amersham).

Indirect immunofluorescence

Strains Y270, Y604, YB115, and YB117 were transformed with YCPF17-*SPH1* and grown to mid-log phase (OD₆₀₀= 1.0) in SC-Trp + 2% galactose medium. Indirect immunofluorescence microscopy was performed as described by Gehring and Snyder (1990). Nonspecific antibodies were removed from the primary and secondary antibodies using formaldehyde-fixed yeast whole cells and spheroplasts (Burns et al., 1994). Spheroplasted cells were washed and incubated with primary antibody overnight at room temperature using anti-HA antibody 16B12. Cells were then treated with secondary antibody for 2 hours at room temperature using CY3-conjugated goat anti-mouse antibodies (Jackson ImmunoResearch, West Grove, PA) and then washed for 5 minutes with PBS/BSA, followed by washes with PBS/BSA + 0.1% NP40 + 0.05% SDS, PBS/BSA + 0.1% NP40, and PBS/BSA. Hoechst 33258 was used to visualize nuclear and mitochondrial DNA. To examine Sph1p localization in pheromone-treated cells, *MATa* cells (Y604) containing YCpIF17-*SPH1* or vector alone were incubated in 5 μ g/ml of α -factor for 60 minutes at 30°C with rotation. A second aliquot of

α -factor that increases the concentration by 5 μ g/ml was added after 1 hour and incubations were continued for 60 minutes. Cells were viewed using a Zeiss Aristoplan and photographed using TMAX400 film.

Mating projection, haploid invasive growth, pseudohyphal growth, and budding pattern analysis

To quantitate mating projection morphologies, mid-log phase *MATa* cells were treated with α -factor as described above. Cells were then fixed in 3.7% formaldehyde at 30°C with rotation, washed in water, and resuspended in Tris, pH 7.5, containing 5 μ g/ml fluorescent brightener 28 (Calcofluor White; Sigma). Mating projections were classified into three morphological groups: wild-type (sharply polarized), broad or peanut-shaped (poorly polarized), or round cells (unpolarized). A minimum of 300 pheromone-treated cells were counted for each sample.

Haploid invasive growth was scored as follows: yeast strains were grown on rich yeast medium (YPAD) for 3 days at 30°C. Cells were gently rinsed off the plate under flowing water without manual agitation and each strain was scored for the presence of residual cells immediately following the wash. Pseudohyphal growth on stains grown for 6-7 days at 30°C on SLAD medium was analyzed according to the method of Gimeno and Fink (1994). To examine the invasive nature of pseudohyphal growth, plates were extensively rinsed under a stream of ddH₂O and vigorously rubbed with a gloved hand as described by Liu et al. (1996).

Budding patterns were examined by staining mid-log phase cells with Calcofluor as described above, and quantified according to the classification scheme of Madden and Snyder (1992). The budding pattern of pseudohyphal cells was viewed by growing cells on SLAD plates 6-7 days at 30°C. After rinsing away surface cells, an agar block containing subsurface cells was heated at 100°C for 5 minutes and 10 volumes of water was added. Cells were recovered by centrifugation, washed extensively in deionized water, and then stained with Calcofluor. Only elongated cells whose length was at least two times greater than their width were scored. Budding patterns were classified into two groups: Class I cells form all buds from one pole and lie adjacent to one another (for cells with only a single bud or bud scar, its position was scored relative to the birth scar), Class II cells bud from both poles.

Two-hybrid analysis

Two-hybrid analyses were carried out essentially as described by Xie et al., (1993). Transformed yeast (Y864) cells were patched onto SC medium lacking leucine and histidine (SC-His-Leu) plates and grown overnight before replica plating onto fresh SC-His-Leu plates containing a sterile circle of 3MM filter paper. Replica plates containing filters were incubated at 30°C for overnight and then lysed with chloroform vapors for 15 minutes. Filters containing the lysed cells were then incubated on a X-Gal (5-bromo-4-chloro-3-indolyl- β -D-galactopyranoside) plate (0.1 M NaPO₄, pH 7, and 1 mM MgSO₄ in 1.6% agar with 120 μ g of X-Gal per ml) and incubated at 30°C for 2 hours.

β -galactosidase assays

To test whether *SPH1* and *SPA2* are required for MAPK cascade-dependent signaling during haploid-invasive and pseudohyphal growth, appropriate strains were transformed with pIL30, containing a *FG(TyA)-lacZ* gene fusion which is strictly induced under such conditions (Mosch et al., 1996).

β -Galactosidase assays were performed on extracts from mid-log phase cultures grown in SC-Ura according to the method of Xie et al. (1993). For assays of nitrogen-starved cells, fresh overnight cultures were washed in water, diluted to approximately 500 colony forming units, spread on SLAD plates, and incubated at 30°C for 3 days. Cells were then harvested from plates and washed with water prior to the preparation of extracts (Xie et al., 1993). Assays were performed at

30°C. Activities were expressed as nmole of *O*-nitrophenyl- β -D-galactopyranoside hydrolyzed per minute times mg of protein.

RESULTS

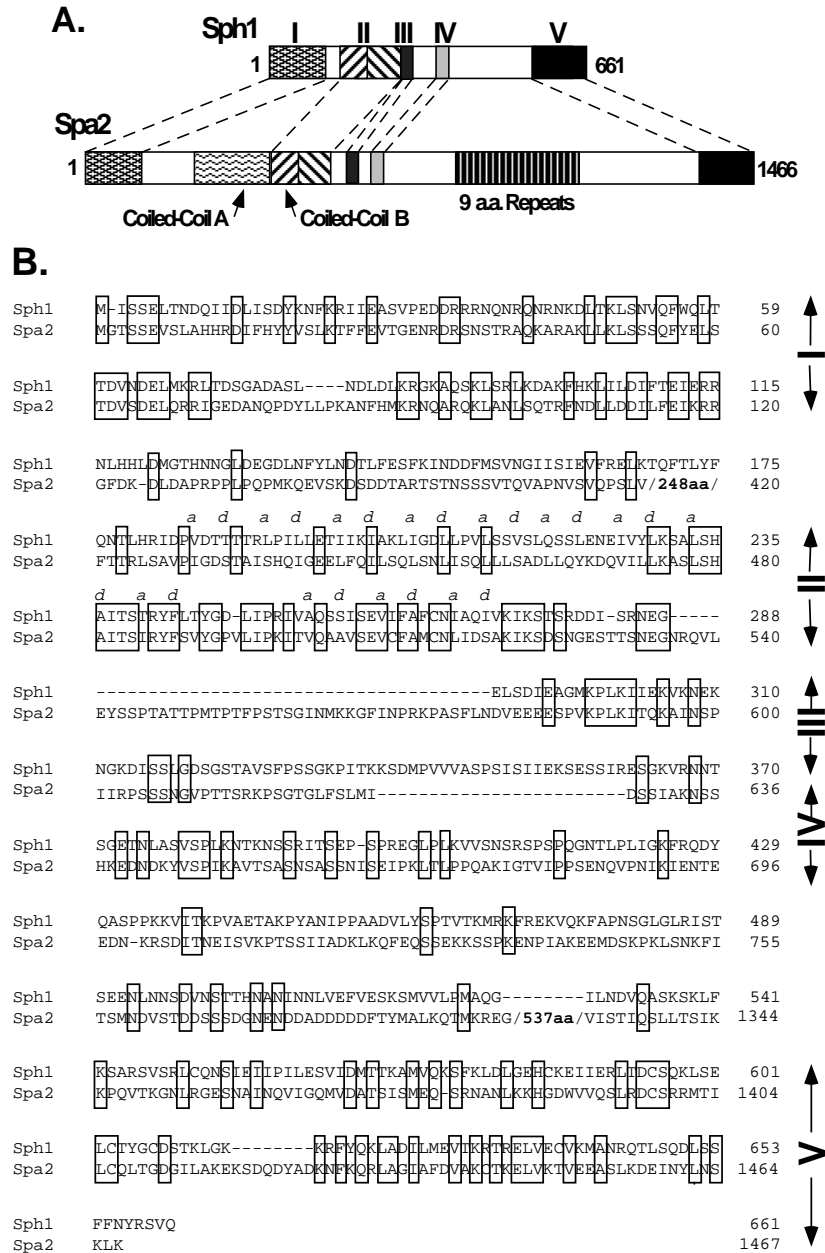
Sph1p is homologous to *Spa2p*

A GenBank homology search using *Spa2p* amino acid sequences identified a *Saccharomyces cerevisiae* open reading frame (ORF) (GenBank accession number U20618/YSC8543.8) which encodes a protein with significant amino acid similarity to *Spa2p* (Fig. 1); this ORF lies immediately downstream of *CDC3* on chromosome XII. We have named this gene *SPH1*, for *SPA2* Homologous gene. The *SPH1* predicted gene product, *Sph1p* (530-661 amino acids, see below), is noticeably smaller than *Spa2p* (1,466 amino acids), and lacks both a coiled-coil region and 9 amino acid repeat domain found in *Spa2p* (Gehring and Snyder, 1990). However, *Sph1p* shares five regions of *Spa2p* homology (domains I through V) which encompass most of the protein. The amino-terminal domain I (amino acids 1-117) and domain II (amino acids 188-288) each share 34% identity with similar regions of *Spa2p* (Fig. 1A,B). Interestingly, domain I contains a 29 amino acid direct repeat element we have called a SDR motif (*SPA2* direct repeat) that shares substantial homology to *H. sapiens* and *C. elegans* proteins (Fig. 1C). Domain II contains a potential leucine zipper-related sequence at amino acid residues 192-272; this coiled-coil type motif facilitates physical interactions between proteins (Steinert and Roop, 1988). Two of the domains (III and IV) are very short (26 and 61 amino acid residues, respectively). Both proteins are also predicted to possess similar carboxyl-terminal domains (34/111 amino acid identity) in most yeast strains examined (Fig. 1, see below).

The *SPH1* sequence in GenBank is predicted to encode a protein of 530 amino acids in length. A potential frameshift in the carboxyl-terminal *SPH1* coding sequence between codons 518 to 530 would lengthen the *SPH1* ORF by 131 codons (Fig. 1D) and extend the homology between *Sph1p* and *Spa2p* to their carboxyl termini. Resequencing of this region of chromosome XII by Johnston et al. (1997) failed to link these two overlapping ORFs. To investigate whether a frameshift might be present in different laboratory strains of yeast, we sequenced PCR fragments spanning the two overlapping ORFs from four different backgrounds, S288C, Σ 1278b, SK1, and W303, as well as PCR fragments from a cDNA library (for details see Materials and Methods). The *SPH1* sequence from S288C, Σ 1278b, and SK1 strains does not contain two guanosines at nucleotide positions 1,582 and 1,583 and therefore contains a long ORF of 1,986 nucleotides encoding a protein of 661 amino acids in each of these strains. In contrast, the W303-derived strain and cDNA library we examined possess alleles of *SPH1* containing the two additional nucleotides thereby encoding a smaller protein (Fig. 1D). Therefore, *SPH1* is polymorphic in different laboratory strains.

SPH1 is important for proper mating projection formation

In order to explore phenotypes associated with the loss of *SPH1*, we deleted 99% of the *SPH1* gene (codons 5 to 658) using the



C.

Sph1	DYKNFKRIIEASVPEDRRRNQNRNNDLTKLSNVQFWQLT	75
Spa2	YVYSLKTFEVTGENRRDSNSTRAQKARAKLLKSSSQFYELSDVSDDELQRRIGEDANQ	76
H. s.	DHKNGQHPFIIIPQADSSLDLSELAKAAKKKLOSLSNHLFEELAMQVYDEVDRRE--TDAVW	298
C. e.	DHKNQDFPIF--EVTEKQFLTKTNDSSRAAISVLPKGGDFDLCEAFDETVRRENEVNW	356

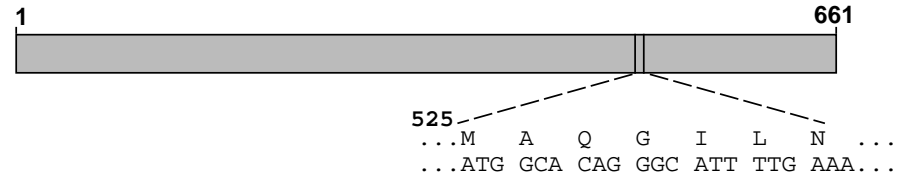
Q N B KL L F L DO EO RR

Sph1	DASLN-----DLDLKRKAQSKLSRLKDAKFKHLILDIFTEIERR	116
Spa2	PDYLL-----PKANFHMKNQAROKLANLSQTRFNDLDDILFEIKRRR	121
H. s.	LATQNHSAIVTETTVVPLFPVNPEYSTRNOGRQKLARFNAHEFATLVIDILSDAKRRQ	356
C. e.	MTKWAKTAKGPTN---LFLPPTPQMSAARNOROKLAKETPIQFTILLIILIKDKORRI	352

Q N B KL L F L DO EO RR

D.

S288C, SK1, Σ 1278b



W303, SPH1-cDNA

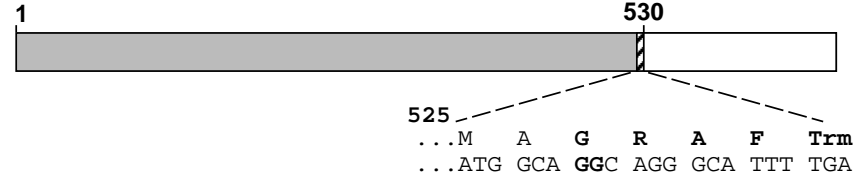


Fig. 1. Sph1p and Spa2p are structurally related and share a region with sequence similarity to *H. sapiens* and *C. elegans* predicted gene products. (A) A schematic comparison of the Sph1p and Spa2p proteins indicates the relative position of five domains (labeled I-V) sharing amino acid sequence similarity. Potential coiled-coil regions and a 9 amino acid repeat domain unique to Spa2p are indicated. (B) Amino acid alignment of Sph1p and Spa2p. The alignment has been optimized by adding gaps (---) to lengthen the Sph1p sequence and deleting two nonhomologous stretches of Spa2p (shown in bold). Domains of homology corresponding to (1A) are indicated as roman numerals. A region of hydrophobic heptad periodicity (coiled-coil domain B) is noted by *a* and *d* symbols above the sequence. Identical residues are boxed. (C) A human cDNA (KIAA0148; accession number D63482) and *C. elegans* gene (F14F3.2; accession number Z49937) are predicted to encode proteins with homologous regions to domain I of Sph1p and Spa2p. Residues common to three or more proteins are in dark shade; residues common to two proteins are lightly shaded. The SPA2 direct repeat element (SDR) common to all four sequences is indicated by arrows. (D) A schematic comparison of two Sph1p isoforms created by the presence or absence of two guanosines (shown in bold) at codon 527. SPH1 from Σ 1278b, SK1, and a subset of S288C strains lack these two nucleotides and encode the full length protein. The GenBank submitted SPH1 sequence (accession number U20618/YSC8543.8) and that of strain W303-A and a cDNA library contain these two nucleotides at codon 527 and truncate the SPH1 protein (shown in bold).

PCR disruption procedure of Baudin et al. (1993; see Materials and Methods). Three independent *sph1Δ1::HIS3/SPH1* heterozygous diploid strains were sporulated and more than 20 tetrads were dissected for each strain. Correct substitution of the *sph1Δ1::HIS3* allele at the genomic locus was verified in each heterozygous diploid and the haploid progeny of two tetrads by PCR analysis. In each case, histidine prototrophy segregated 2His⁺:2His⁻ with no apparent difference in growth rate between wild-type and *sph1Δ1::HIS3* segregants incubated at either 16°, 23°, 30°, or 37°C. Growth in both rich medium (YPAD) and synthetic complete medium (SC) were tested at each temperature. To examine the genetic relationship between *SPH1* and *SPA2*, a *sph1Δ1::HIS3/SPH1 spa2Δ2::TRP1/SPA2* double heterozygous diploid strain was constructed and sporulated. No difference in growth rate was detected in haploid *sph1Δ1::HIS3 spa2Δ2::TRP1* double mutants compared to either single mutants or isogenic wild-type strains at the various temperatures and media conditions described above. Diploids homozygous for *sph1Δ1::HIS3* or both *sph1Δ1::HIS3* and *spa2Δ2::TRP1* also grew at rates indistinguishable from those of an isogenic wild-type diploid strain. Thus, neither *SPH1* nor the *SPH1-SPA2* gene pair are essential for vegetative growth.

Cells carrying a *sph1*-deletion were examined for a variety of morphological and polarity defects common to *spa2*-disrupted cells. Unlike *spa2Δ2::TRP1/spa2Δ2::TRP1* diploid cells, which appear round, *sph1Δ1::HIS3/sph1Δ1::HIS3* cells and wild-type diploid cells are both clearly ellipsoidal. *spa2Δ* cells also display a diploid-specific budding pattern defect. *spa2Δ/spa2Δ* daughter cells (i.e. cells which have yet to bud) initiate their first bud from the distal pole similar to wild-type cells. This tendency to bud from the distal tip (the pole opposite the birth pole) in diploid daughter cells is referred to as a distal tip bias (Friefelder, 1960; Snyder, 1989; Chant and Pringle, 1995). However, unlike wild-type cells which eventually bud from both poles, diploid *spa2Δ/spa2Δ* cells bud in a progressively random fashion in subsequent budding cycles (Snyder, 1989; Zahner et al., 1996). Budding pattern defects were not detected in either S288C or Σ1278b haploid or diploid strains deleted for *SPH1* (Table 2). In addition, a S288C diploid strain homozygous for both *sph1Δ1::HIS3* and *spa2Δ2::TRP1* does not disrupt the distal tip budding bias preserved in *spa2Δ/spa2Δ* daughter cells (data not shown).

Haploid *spa2* mutants are unable to form properly polarized growth projections in the presence of mating pheromone and, depending upon conditions, form oval cells or cells with broad mating projections (Gehring and Snyder, 1990; Chenevert et al., 1994; Yorihuzi and Ohsumi, 1994; Valtz and Herskowitz, 1996). Cells deleted for *sph1* were similarly analyzed for a mating projection defect. When exposed to a high isotropic concentration of the α-factor mating pheromone, *sph1Δ1::HIS3* cells exhibit a mild polarization defect and usually form projections that are slightly broader at the base and rounder at the tip (Fig. 2A,B). This morphology approaches the 'peanut'-shaped morphology described previously for both *spa2* and *pea2* mutants (Chenevert et al., 1994; Yorihuzi and Ohsumi, 1994), but is clearly less pronounced than that observed for *spa2* cells (Fig. 2C). However, *sph1Δ1::HIS3 spa2Δ2::TRP1* double mutants display an exaggerated mating projection morphology defect that appears more severe than that observed for either single mutant (Fig. 2D). Classification of the various mating projection morphologies into the three groups, normal, broad

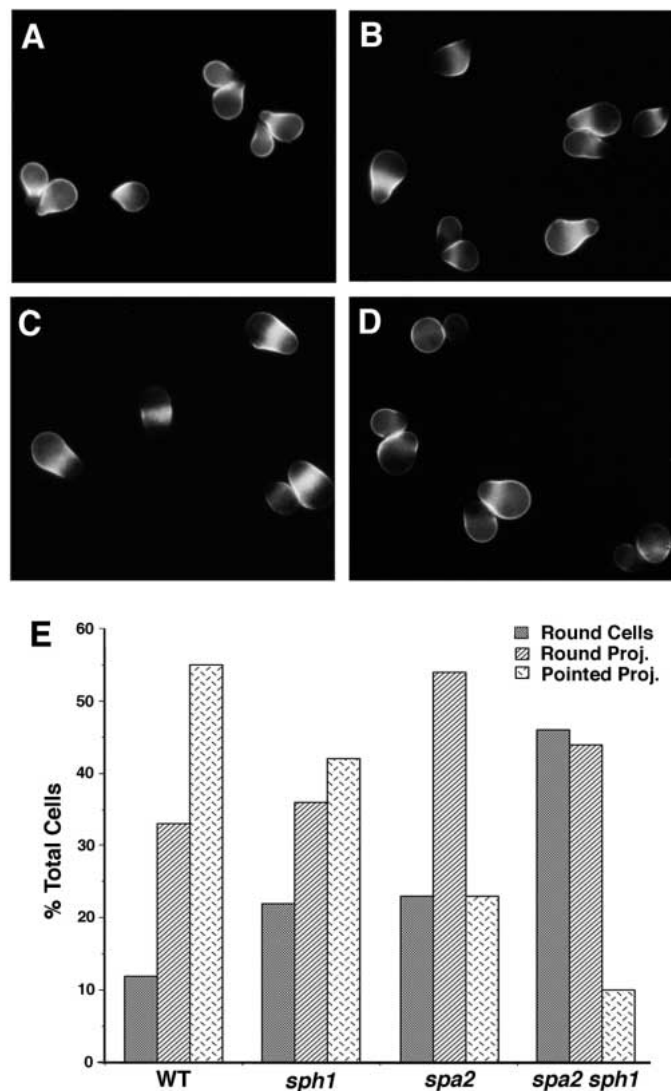


Fig. 2. Mating projection defects of *sph1* mutants. Haploid *MATa* cells that were (A) wild-type (Y1284), (B) *sph1Δ* (Y1283), (C) *spa2Δ* (Y1292) and (D) *sph1Δ spa2Δ* (Y1281), were treated with α-factor, fixed, and stained with Calcofluor which binds chitin at the base of the projection (see Materials and Methods for details). (E) Quantitative analysis of mating projection morphologies in wild-type, *sph1Δ*, *spa2Δ*, and *sph1Δ spa2Δ* double mutants. Seen is the graphic representation of the percentage of total α-factor-treated cells counted from 2-3 different strains for each genotype classified as to mating projection morphology. More than 700 cells were counted for each genotype.

tip or peanut-shaped, and round cells, revealed that a significantly higher proportion of *sph1Δ1::HIS3 spa2Δ2::TRP1* double mutants fail to form projections when compared to either single mutant (Fig. 2E). This is not attributed to an impaired sensitivity to α-factor since all strains yield α-factor halos (impaired zones of cell growth) comparable to wild-type cells (data not shown). Thus, *SPH1* contributes to projection formation in yeast and may be functionally redundant with *SPA2*. Consistent with this possibility, although *sph1Δ* mutants lack a quantitative mating defect, overexpression of *SPH1* partially restores mating efficiency in *spa2Δ* cells (Arkowitz and Lowe, 1997).

Table 1. List of strains used in this study

Strain	Genotype	Background/source
Y270	<i>MATa/MATα ura3-52/ura3-52 lys2-801/lys2-801 ade2-101/ade2-101 trp1-Δ1/trp1-Δ1 his3-Δ200/his3-Δ200</i>	
Y602	<i>MATa ura3-52 lys2-801 ade2-101 trp1-Δ1 his3-Δ200 spa2Δ3::URA3</i>	
Y604	<i>MATa ura3-52 lys2-801 ade2-101 trp1-Δ1 his3-Δ200</i>	
Y824	<i>MATa/MATα leu2::HISG/leu2::HISG ura3-52/ura3-52</i>	Σ1278b/G. Fink, MIT, Cambridge, MA
Y825	<i>MATa leu2::HISG ura3-52</i>	Σ1278b/G. Fink, MIT, Cambridge, MA
Y826	<i>MATα leu2::HISG ura3-52</i>	Σ1278b/G. Fink, MIT, Cambridge, MA
Y864	<i>MATa leu2-3,112 ura3-52 ade2-101 trp1-901 his3-Δ200 gal4Δ gal80Δ plexA-lacZ-URA3</i>	
Y1146	<i>MATα leu2::HISG ura3-52 spa2Δ3::URA3</i>	Σ1278b
Y1149	<i>MATa leu2::HISG ura3-52 spa2Δ3::URA3</i>	Σ1278b
Y1173	<i>MATa leu2::HISG ura3-52 sph1Δ2::LEU2</i>	Σ1278b
Y1174	<i>MATα leu2::HISG ura3-52 sph1Δ2::LEU2</i>	Σ1278b
Y1175	<i>MATa leu2::HISG ura3-52 sph1Δ2::LEU2 spa2Δ3::URA3</i>	Σ1278b
Y1176	<i>MATα leu2::HISG ura3-52 sph1Δ2::LEU2 spa2Δ3::URA3</i>	Σ1278b
Y1177	<i>MATa/MATα leu2::HISG/leu2::HISG ura3-52/ura3-52 sph1Δ2::LEU2/sph1Δ2::LEU2 spa2Δ3::URA3/spa2Δ3::URA3</i>	Σ1278b
Y1281	<i>MATa ura3-52 lys2-801 ade2-101 trp1-Δ1 his3-Δ200 spa2Δ2::TRP1 sph1Δ1::HIS3</i>	
Y1282	<i>MATa ura3-52 lys2-801 ade2-101 trp1-Δ1 his3-Δ200 sph1Δ1::HIS3</i>	
Y1284	<i>MATa ura3-52 lys2-801 ade2-101 trp1-Δ1 his3-Δ200</i>	
Y1292	<i>MATa ura3-52 lys2-801 ade2-101 trp1-Δ1 his3-Δ200 spa2Δ2::TRP1</i>	
Y1340	<i>MATa/MATα leu2::HISG/leu2::HISG ura3-52/ura3-52 sph1Δ2::LEU2/sph1Δ2::LEU2 pRS415</i>	Σ1278b
Y1345	<i>MATa/MATα leu2::HISG/leu2::HISG ura3-52/ura3-52 spa2Δ1::URA3/spa2Δ3::URA3 pRS415</i>	Σ1278b
S2065	<i>MATa/MATα leu2-hisG/leu2-hisG ho-LYS2/ho-LYS2 ura3/ura3</i>	SK1/S. G. Roeder, Yale U., New Haven, CT
W303-A	<i>MATα ade2 can1-100 his3-11,115 leu2-3,112 trp1-1 ura3-1</i>	R. Rothstein, Columbia U., New York, NY
Y1213	<i>MATa leu2-3,112 ura3-52 ade2-101 trp1-901 his3-Δ200 galΔ gal80Δ ste5Δ plexA-lacZ-URA3</i>	Y-J Sheu, Yale New Haven, CT
Y1214	<i>MATa/MATα leu2-3,112/ leu2-3,112 ura3-52 /ura3-52 his3-Δ200/his3-Δ200 trp1-Δ1/trp1-901 suc2-Δ9/suc2-Δ9 lys2-801/LYS2 ade2/ADE2</i>	SEY6210 × SEY6211
Y1215	<i>MATa/MATα leu2-3,112/ leu2-3,112 ura3-52 /ura3-52 his3-Δ200/his3-Δ200 trp1-Δ1/trp1-901 suc2-Δ9/suc2-Δ9 lys2-801/LYS2 ade2/ADE2 sph1Δ1::HIS3/ sph1Δ1::HIS3</i>	
SEY6210	<i>MATα leu2-3,112 ura3-52 his3-Δ200 trp1-901 suc2-Δ9 lys2-801</i>	H. Bussey, McGill Montreal. Queb.
SEY6211	<i>MATa leu2-3,112 ura3-52 his3-Δ200 trp1-901 suc2-Δ9 ade2</i>	H. Bussey, McGill Montreal. Queb.
YB115	<i>MATa/MATα ura3-52/ura3-52 LEU2/leu2-Δ98 lys2-801/lys2-801 ade2-101/ade2-101 trp1-Δ1/trp1-901 his3-Δ200/HIS3</i>	
YB117	<i>MATa/MATα ura3-52/ura3-52 LEU2/leu2-Δ98 lys2-801/lys2-801 ade2-101/ade2-101 trp1-Δ1/trp1-901 his3-Δ200/HIS3 spa2Δ3::URA3/spa2Δ3::URA3</i>	

All strains are in the S288C background unless otherwise noted.

SPH1 and SPA2 are required for pseudohyphal growth

Haploid invasive growth and pseudohyphal growth rely on

Table 2. Budding pattern of *sph1* Δ/*sph1* Δ diploid cells

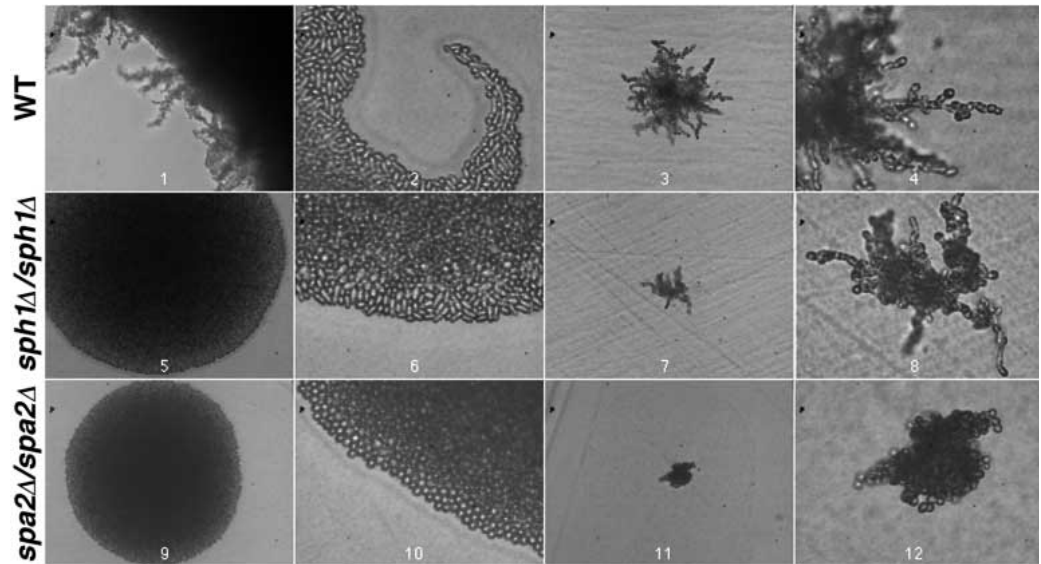
Class	Relevant genotype	Distal (%)	Random (%)	Proximal (%)
1 bud scar	Wild type	100	0	0
	<i>sph1</i> Δ/ <i>sph1</i> Δ	100	0	0
2 bud scars	Wild type	100	0	0
	<i>sph1</i> Δ/ <i>sph1</i> Δ	95	0	5
3 bud scars	Wild type	20	0	80
	<i>sph1</i> Δ/ <i>sph1</i> Δ	25	0	75
4 bud scars	Wild type	69	6	25
	<i>sph1</i> Δ/ <i>sph1</i> Δ	69	2	29
≥ 5 bud scars	Wild type	86	9	5
	<i>sph1</i> Δ/ <i>sph1</i> Δ	90	5	5

Cells with one or two bud scars were scored relative to the birth scar. The positions of bud scars were scored as distal pole (the third of the cell distal the birth scar), random (at least one bud scar in the middle of the cell), or proximal pole (the third of the cell adjacent the birth scar). Cells with 3 or more bud scars were scored relative to one another with distal sites referring to at least one bud scar at each pole, and proximal sites referring to all bud scars concentrated at one pole. Between 100 and 200 cells were scored for each class. The strains analyzed are wild type (Y1214), and *sph1* Δ/*sph1* Δ (Y1215) in the strain background of Arkowitz and Lowe (1997).

polarized growth mechanisms in yeast including cell elongation and bud site selection and, therefore, serve as a sensitive *in vivo* measure for polarity defects. To explore a role for *SPH1* and *SPA2* in haploid invasive growth and pseudohyphal growth, both genes were disrupted in Σ1278b, a strain background capable of both these processes (see Materials and Methods for details). Neither *sph1*Δ, *spa2*Δ nor *sph1*Δ *spa2*Δ mutants in this second strain background display any noticeable growth defect relative to wild type under the different vegetative conditions tested (see above).

Diploid *spa2*Δ/*spa2*Δ, *sph1*Δ/*sph1*Δ, and *spa2*Δ/*spa2*Δ *sph1*Δ/*sph1*Δ Σ1278b mutants were first analyzed for defects in pseudohyphal growth. Diploid cells deleted for *spa2* when grown under nitrogen-limiting conditions, fail to form pseudohyphal filaments, unlike wild-type diploid Σ1278b cells which form complex pseudohyphal filaments extending beyond and directly below the colony (Fig. 3, panels 1,3). Instead, *spa2*-deleted colonies form small subsurface aggregates of cells directly below the center of the colony, without ever forming filaments either away or under the colony (Fig. 3, panels 11,12). While other parts of our study of *SPH1* were being completed, Mosch and Fink (1997) reported that an insertional mutation in *SPA2*, which truncates the protein after amino acid 995, causes defects in budding pattern, cell shape and invasive growth during pseudohyphal development.

Fig. 3. *SPA2* and *SPH1* are important for pseudohyphal growth. $\Sigma 1278b$ wild-type strain, Y824 (1-4), $\Sigma 1278b$ *sph1* Δ /*sph1* Δ (Y1340) (5-8), and $\Sigma 1278b$ *spa2* Δ /*spa2* Δ (Y1345) (9-12) strains were grown for 7 days at room temperature on SLAD medium and both pre-washed (1,2,5,6,9,10) and post-washed (3,4,7,8,11,12) colonies were examined (see Materials and Methods). Representative colonies and cells are shown. Panels 1,5,9 are the same magnification as 3,7,11. Panels 2,4,6,8,10,12 are an enlargement of the colonies seen in 1,3,5,7,9,11, respectively.



We also observe these phenotypes, although we detect a more extreme defect in *spa2* Δ /*spa2* Δ cells efficiently penetrating the agar. This is particularly evident in colonies grown for a shorter period of time (e.g. 3 days; data not shown). A striking cell morphology defect is also evident for $\Sigma 1278b$ *spa2* Δ /*spa2* Δ cells; they remain round and fail to elongate like wild-type cells after prolonged growth on limiting nitrogen (Fig. 3, panels 10,12; see Fig. 4). Budding patterns of pseudohyphal *spa2* Δ /*spa2* Δ cells that had invaded the agar were assessed by visualizing the chitin-rich bud scars on subsurface cells stained with the chitin binding dye, Calcofluor White (see Materials and Methods). As reported for vegetatively growing diploid *spa2* Δ /*spa2* Δ strains, *spa2* Δ /*spa2* Δ cells on nitrogen-limiting SLAD medium exhibit a random budding pattern (Fig. 4).

Surprisingly, an examination of budding pattern for a population of wild-type $\Sigma 1278b$ diploid cells growing invasively on SLAD plates did not reveal a unipolar mode of bud site selection; instead, a bipolar budding pattern was observed (Figs 4, 5). Quantitation of site selection in new mother cells (i.e. cells which have undergone one budding event) indicates a bipolar mode of bud site selection similar to vegetative cells (Snyder, 1989; Kron et al., 1994; Chant and Pringle, 1995); 29% of cells contain a bud scar at each pole. Moreover, examination of older mother cells (i. e. cells possessing three or more bud scars) revealed 82% of cells display at least one bud scar at the pole opposite that predicted from a unipolar budding pattern (Fig. 5A). Consistent with these observations, examination of the budding pattern in the same $\Sigma 1278b$ diploid strain maintaining 2 μ copies of *PHD1*, *PHD2*, or *MCM1*, three genes capable of enhancing the pseudohyphal filament formation (Gimeno and

Fink, 1994; our unpublished observations) reveal strikingly similar budding pattern profiles; namely a strong trend towards bipolar budding correlating with the number of budding events

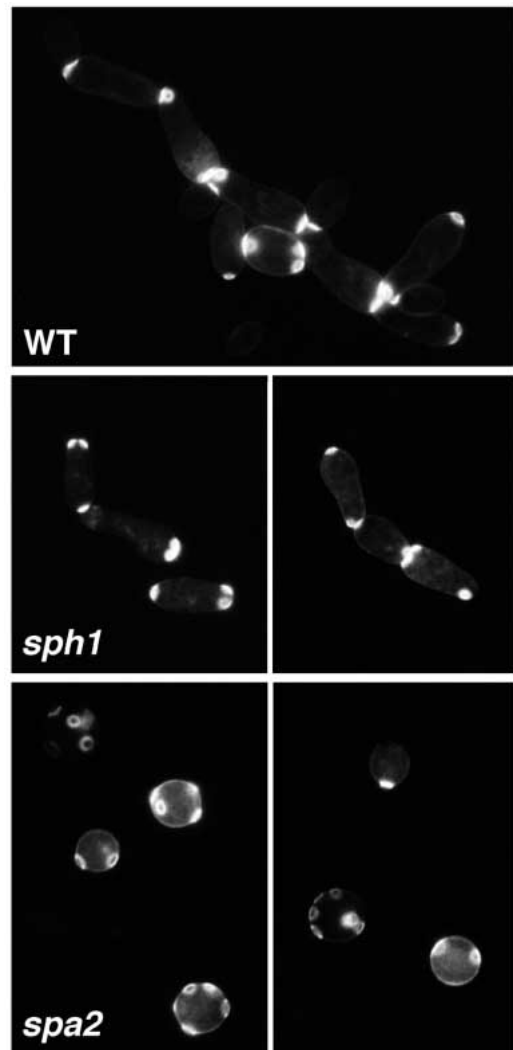


Fig. 4. Budding pattern of $\Sigma 1278b$ diploids. (A) Wild type (Y824), (B) *sph1* Δ /*sph1* Δ (Y1340), and (C) *spa2* Δ /*spa2* Δ (Y1345) incubated on SLAD medium. Cells were incubated 7 days on plates at room temperature, extracted from the agar (see Materials and Methods), and stained with Calcofluor to visualize bud scars. Wild-type and *sph1* Δ /*sph1* Δ filaments typically possess elongated cells bearing bud scars from both poles (bipolar pattern). *spa2* Δ /*spa2* Δ cells fail to form filaments and remain round with bud scars positioned randomly.

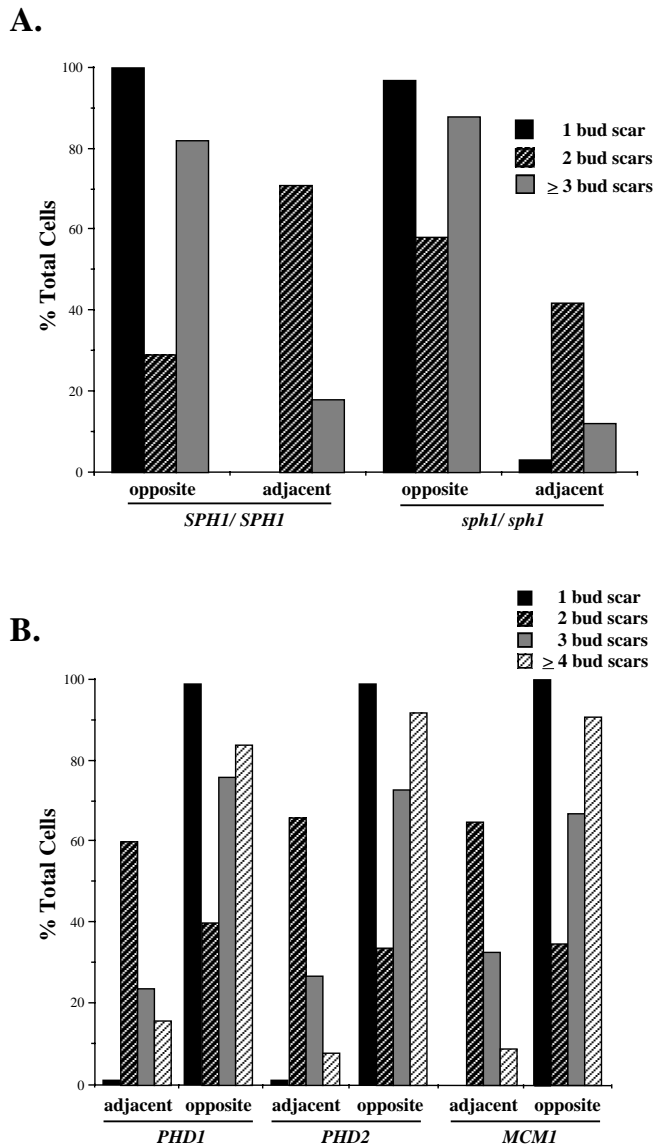


Fig. 5. Pseudohyphal cells choose bipolar sites in successive budding events. Budding pattern was determined from cells incubated on SLAD plates for 6 days at 30°C, extracted from the agar and Calcofluor stained (See Materials and Methods for details). (A) The position of the first bud or bud scar in Y824 (*SPH1/SPH1*) and Y1340 (*sph1Δ/sph1Δ*) was scored as either opposite or adjacent to the birth scar pole. In older cells (≥ 2 budding events), the position of the bud or bud scar was scored relative other bud scar(s); budding events were scored as occurring either from opposite poles, or adjacent to one another at one pole. Approximately 600 cells were counted for each strain. (B) Bud site selection of pseudohyphal cells (*Y824*) maintaining multicopy plasmids of *PHD1*, *PHD2*, or *MCM1*. Approximately 300 cells were scored as above (A) for bud position for each strain.

completed (Fig. 5B). As described previously for pseudohyphal cells (Gimeno and Fink, 1994; Kron et al., 1994), analysis of the budding pattern in new daughter cells demonstrates an extreme bias for bud formation at the distal tip; this distal tip bias is also normally observed in vegetatively growing diploid daughter cells (Friefelder, 1960; Chant and Pringle, 1995).

Homozygous *sph1Δ/sph1Δ* cells are also partially defective

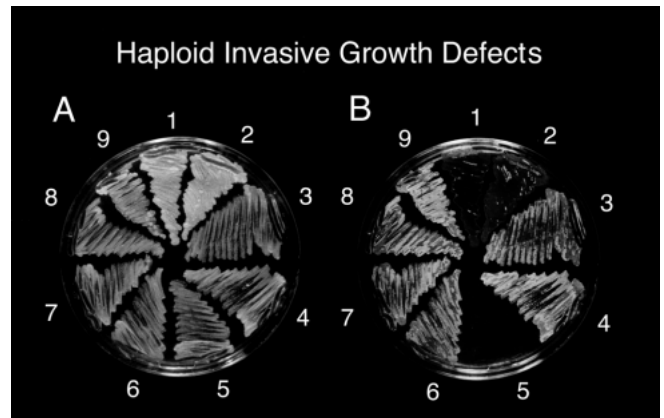


Fig. 6. Haploid invasive growth is impaired in *sph1Δ spa2Δ* cells. (A) A YPAD plate containing the following $\Sigma 1278b$ strains: (1) *MATa sph1Δ spa2Δ* (Y1175), (2) *MAT α sph1Δ spa2Δ* (Y1176), (3) *MATa SPH1 SPA2* (Y825), (4) *MAT α SPH1 SPA2* (Y826), (5) *MATa/ α SPH1/SPH1 SPA2/SPA2* (Y824), (6) *MATa SPH1 spa2Δ* (Y1149), (7) *MAT α SPH1 spa2Δ* (Y1146), (8) *MATa sph1Δ SPA2* (Y1173), and (9) *MAT α sph1Δ SPA2* (Y1174). Cells were incubated at 30°C for 3 days and photographed. (B) The same plate after gently rinsing with deionized water. Wild-type haploid (3,4) and diploid (5) strains provide positive and negative controls, respectively, for haploid invasive growth.

in pseudohyphal growth by three criteria. Unlike wild-type $\Sigma 1278b$ cells which form many pseudohyphae that extend away from the colony perimeter, $\Sigma 1278b$ *sph1Δ/sph1Δ* cells rarely radiate filaments from the colony (Fig. 3, compare panels 1,5). *sph1Δ/sph1Δ* cells develop pseudohyphal filaments; however, agar penetration of these filaments appears impaired and the invasive pseudohyphal networks that remain on washed plates are less complex (Fig. 3, compare panels 3,4,7,8). *sph1/sph1* cells do develop an elongated morphology indistinguishable from wild-type cells when grown under nitrogen-limiting conditions (Figs 3, 4). *sph1Δ/sph1Δ* cells also exhibit a modest defect in budding patterns under conditions of limiting nitrogen (Fig. 5A), and exhibit a twofold increase in the frequency of bud site selection to the proximal pole in *sph1Δ/sph1Δ* new mother cells relative to wild-type $\Sigma 1278b$ cells. No significant difference between *sph1Δ/sph1Δ* cells and $\Sigma 1278b$ cells was observed in bud-site preference for new daughter or older mother cells. The tendency to choose the proximal pole approximately one budding cycle earlier than wild-type cells is consistent with the less complex pseudohyphal filaments and denser colony growth characteristic of $\Sigma 1278b$ *sph1Δ/sph1Δ* cells. Construction of a *sph1Δ/sph1Δ spa2Δ/spa2Δ* mutant in the $\Sigma 1278b$ strain background (see Materials and Methods) resulted in pseudohyphal phenotypes indistinguishable from the *spa2Δ/spa2Δ* homozygous mutant.

Cells containing either *sph1Δ*, *spa2Δ*, and *sph1Δ spa2Δ* double mutants were also examined for defects in haploid invasive growth. Cells of both mating types were incubated on YPAD plates for 3 days at 30°C. Plates were photographed before and after a gentle rinse with distilled water. Wild-type cells readily invade the agar and grow back on the plate after washing. As shown in Fig. 6, *sph1Δ2::LEU2 spa2Δ3::URA3* cells display an impairment in haploid invasive growth

approaching the complete absence of haploid invasive growth characteristic of wild-type diploid cells. The residual level of invasive growth detected in *sph1Δ spa2Δ* cells is similar to that observed for *ste11Δ*, *ste7Δ*, and *ste12Δ* mutations in the pheromone response pathway (Roberts and Fink, 1994). Thus, *SPH1* and *SPA2* are each important for pseudohyphal growth and together are required for haploid invasive growth.

Sph1p localizes to polarized growth sites in vegetative and mating cells

To begin to characterize the *SPH1* gene product, *SPH1* was tagged at its carboxyl-terminal coding sequences in the genomic locus of a S288C strain with a DNA segment encoding three copies of the influenza hemagglutinin (HA) epitope (Schneider et al., 1995). Immunoblot analysis with anti-HA antibodies reveal a weakly staining Sph1::3XHA band at the expected molecular mass of approximately 80 kDa, indicating that the protein is present at a low level (data not shown). Indirect immunofluorescence experiments failed to detect Sph1::3XHA localization under a variety of conditions tested. To enhance detection of Sph1p, Sph1p expression was placed under the control of the *GALI* promoter and tagged at its amino terminus with a single HA epitope (see Materials and Methods). Immunoblot analysis with anti-HA antibodies detect the conditional expression of Sph1::1XHA in both haploid and diploid strains grown in medium containing galactose; the protein migrates very close to its expected size of 77 kDa (Fig. 7). Similar to results reported for Pea2p, Sph1::1XHA appears to be slightly unstable in *spa2*-deleted cells; a collection of degradation products are reproducibly more pronounced in *spa2* cells than in wild-type cells (Fig. 7, lanes 6,7).

To determine the subcellular localization of Sph1p, cells transformed with either the Sph1::1XHA plasmid or vector alone and grown in galactose medium were examined using

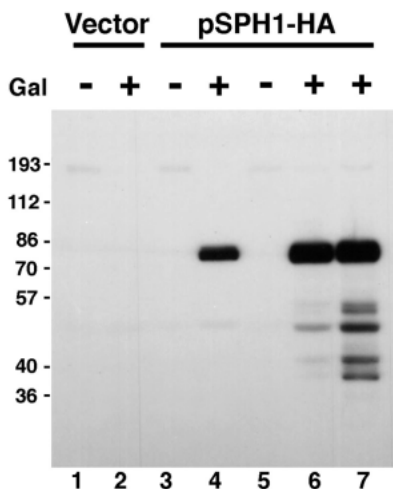


Fig. 7. Immunoblot analysis of Sph1::1XHA in wild-type and *spa2Δ* cells. Sph1::1XHA was detected by immunoblot analysis of protein extracts from diploid strain Y270 grown in glucose (–) or galactose (+) and maintaining either YCpIF17 vector alone (lanes 1,2), or the YCpIF17-Sph1::1XHA plasmid (lanes 3,4). Immunoblots were probed with anti-HA antibodies. Proteins were also analyzed from the wild-type haploid strain Y602 (lanes 5,6) and *spa2Δ* deleted strain, Y604 (lane 7). Enhanced degradation of Sph1p was detected in *spa2Δ* cells in three independent experiments.

indirect immunofluorescence methods. Sph1p localizes to sites of polarized growth in both haploid (data not shown) and diploid vegetatively growing cells (Fig. 8). Sph1p is localized in a cell cycle-specific manner similar to Spa2p and a variety

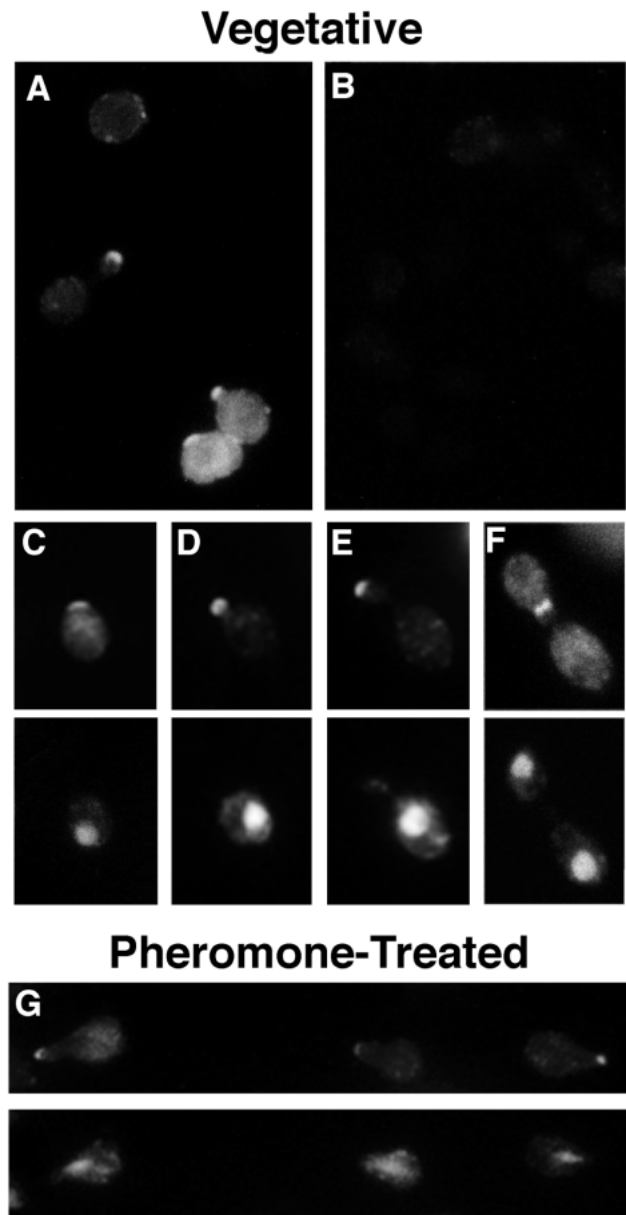


Fig. 8. Sph1p localizes to sites of polarized growth in vegetative and pheromone-treated cells. (A,B) Diploid cells (Y270) containing Sph1::1XHA (A) or vector alone (B) were stained with anti-HA antibody 16B12 and examined by indirect immunofluorescence. (C-F) Examples of Sph1::1XHA-stained cells at different stages of the cell cycle. Hoechst 33258 staining of the nucleus for each of these cells is shown in the lower panel. (C) An unbudded cell with staining concentrated as a patch near the cell cortex. (D) A small-budded cell showing Sph1p staining around the bud periphery. (E) Sph1p is concentrated to the bud tip in medium-sized budded cells. (F) In large-budded cells undergoing cytokinesis, Sph1p staining is detected at the bud neck. (G) *MATa* cells (Y604) containing Sph1::1XHA (top) or vector alone (not shown) were treated with α -factor and stained with anti-HA antibody. Sph1p concentrates at the tip of the mating projection. Lower panel shows Hoechst staining of nuclei in the same cells.

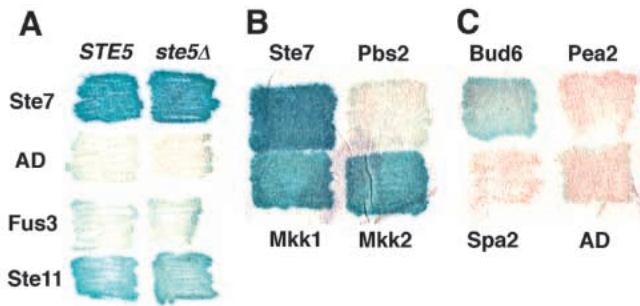


Fig. 9. Sph1p interacts with MAP kinase components and the polarity protein, Bud6p by the two-hybrid system. (A) Sph1-DBD interacts strongly with Ste7-AD and Ste11-AD in both *STE5* (Y864) and *ste5Δ* (Y1213) strain backgrounds. A slight interaction above background is also detected between Sph1-DBD and Fus3-AD. AD, activating domain vector. (B) Sph1-DBD interacts with additional MAPKKs including Mkk1-AD and Mkk2-AD. (Note: quantitation of these interactions reveals Sph1-DBD interacts more strongly with Mkk1-AD than Mkk2-AD; Table 3.) However, no interaction is detected between Sph1-DBD and Pbs2-AD. (C) Sph1-DBD also interacts weakly with a Bud6p fragment (amino acids 275-788) fused to the *GAL4* activation domain. No interaction is seen with either Pea2p or Spa2p. β -Galactosidase levels measured for all the above interactions as well as additional interactions not pictured here are presented in Table 3.

of other polarity proteins. Sph1p is detected in unbudded cells as either a broad or narrow patch associated with the cell cortex (40% of cells; $n=297$) (Fig. 8C). This localization is likely to correspond to the incipient bud site or the site of cytokinesis, since in diploid cells (in which the poles are more easily inferred from their elongated shape), the Sph1p patch localizes to one end of the cell. A single Sph1p patch is typically observed at one pole of the cell, although a very small fraction of diploid cells (1% of cells; $n=297$) exhibit Sph1p staining at both poles. Sph1p is most readily detected in small-budded cells (95% of cells; $n=205$), where it accumulates in the distal half of the bud (Fig. 8D). In medium-budded cells, Sph1p remains localized to the bud (84% of cells counted; $n=214$), and is most concentrated at the extreme bud tip (Fig. 8E). Finally, Sph1p localizes to the mother-bud neck in large-budded cells that have two separated nuclei and are preparing for cytokinesis (43% of cells counted; $n=102$) (Fig. 8F).

Because the localization of Sph1p is strikingly similar to Spa2p during vegetative growth and *spa2Δ sph1Δ* cells display an exaggerated morphology defect during mating, we examined Sph1p localization in cells treated with mating pheromone. As shown in Fig. 8G, Sph1p concentrates at the projection tip in α -factor treated cells (>99% of cells counted; $n=295$). However, unlike Spa2p which typically localizes as a broad patch spanning the entire tip, only those cells strongly overexpressing Sph1p display a localization resembling a Spa2p patch (data not shown). Increased expression of Sph1::3XHA was not observed in pheromone-treated extracts by immunoblot analysis (data not shown).

Since the localization of Sph1p and Spa2p are similar, we tested whether Spa2p affects Sph1p localization in vegetative or mating cells. Although Spa2p is not essential for Sph1p localization, its absence significantly affects the Sph1p staining pattern. This is most apparent in cells with a mating projection,

in which approximately 15% of *spa2Δ* cells reveal Sph1p staining compared to 99% of wild-type cells. Moreover, those *spa2Δ* cells that stain with Sph1p exhibit very faint staining in contrast to the wild-type cells which display strong tip staining. Because *spa2Δ* mutations affect shmoo morphology, Sph1p localization pattern was also quantified in vegetatively growing *spa2*-deleted cells. A substantial reduction in the frequency of detectable Sph1p staining was observed at all stages of the cell cycle in *spa2* cells: unbudded cells (8% ($n=251$) vs 40%), small-budded cells (35% ($n=205$) vs 95%), medium-budded cells (14% ($n=234$) vs 84%), and large-budded cells (12% ($n=112$) vs 43%). Thus Spa2p contributes to the proper localization of Sph1p.

Two-hybrid analysis reveals Sph1p interacts with MAP kinase signaling molecules

Y.-J. Sheu et al. (unpublished observations) describe data that indicate that Spa2p interacts with two distinct classes of proteins: (1) constituents of MAP kinase modules, and (2) polarity components. To examine whether Sph1p interacts with either of these classes of molecules, we have utilized the two-hybrid system (Fields and Song, 1989; Zervos et al., 1993). Full length Sph1p interacts strongly and specifically with Ste7p in the two-hybrid assay when fused either to the *lexA* DNA-binding domain (DBD) or Gal4p activation domain (AD) (Fig. 9A,B; Table 3). (Note: a low level of background staining is produced by either Sph1- or Ste7-*lexA* fusion proteins alone, a feature often observed with other *lexA* fusion proteins.) Sph1-DBD also interacts strongly with Ste11-AD. Unlike the above interaction between Sph1p and Ste7p, no interaction was detected in the reciprocal test using Sph1-AD and Ste11-DBD (Table 3). To further examine the specificity of the interaction between Sph1p and Ste7p and Ste11p, we also tested whether Sph1p interacts with additional components of this MAP kinase module. No significant two-hybrid interaction were detected between Sph1p and DNA-binding fusions of the PAK65 homolog, Ste20p. However, a very modest two-hybrid interaction between Sph1p and the MAP kinase, Fus3p was reproducibly detected (Fig. 9A; Table 3).

To determine whether the interactions between Sph1p and both Ste7p and Ste11p are potentially mediated by STE5p, a putative scaffold protein, these two-hybrid interactions were additionally analyzed in a background deleted for *STE5*. No significant difference in the interactions between Sph1-DBD and Ste7-AD or the reciprocal Sph1-AD and Ste7-DBD combination were detected in this strain background relative to the wild-type strains (Fig. 9A; Table 3). Similarly, the two-hybrid interaction detected between Sph1-DBD and Ste11-AD is unaffected in a *ste5*-deleted mutant.

Genetic evidence demonstrates that the *SPA2* gene product plays a role in a second MAP kinase pathway involved in cell wall integrity and actin cytoskeleton dynamics (see Discussion). Y.-J. Sheu et al. (unpublished observations) demonstrate that Spa2p interacts with each of the two MAPKKs involved in this signaling cascade. Similarly, we detect two-hybrid interactions between Sph1-DBD and either Mkk1-AD or Mkk2-AD (Fig. 9B; Table 3). Interestingly, Sph1p can discriminate between different MAPKKs since Sph1-DBD does not interact with Pbs2p, the MAPKK component of the HOG MAP kinase pathway involved in the response to high osmotic shock. Other components of the

Table 3. Summary of two-hybrid interactions

Relevant genotype	DNA-binding domain fusion	Activation domain fusion	β -Galactosidase activity*
<i>STE5</i>	Sph1†	Ste7	986±315
<i>ste5Δ</i>	Sph1	Ste7	560±119
<i>STE5</i>	Ste7	Sph1	231±44
<i>ste5Δ</i>	Ste7	Sph1	142±7.3
<i>STE5</i>	Sph1	Ste11	24.3±2.9
<i>ste5Δ</i>	Sph1	Ste11	29.3±7.7
<i>STE5</i>	Ste11	Sph1	2.6±0.9
<i>ste5Δ</i>	Ste11	Sph1	2.0±0.8
<i>STE5</i>	Sph1	Fus3	6.2±1.4
<i>ste5Δ</i>	Sph1	Fus3	6.1±1.2
<i>STE5</i>	Fus3†	Sph1	3.7±0.7
<i>ste5Δ</i>	Fus3	Sph1	2.6±2.2
<i>STE5</i>	Sph1†	Mkk1	440±102
	Sph1†	Mkk2	21.2±2.5
	Sph1†	Pbs2	2.5±0.7
	Sph1	Slt2	8.5±2.4
	Slk1	Sph1	2.0±0.7
<i>STE5</i>	Sph1†	Bud6 ₍₂₇₅₋₇₈₈₎	106±17
	Sph1	Bud6 ₍₃₅₈₋₇₆₆₎	7.2±1.2
	Sph1†	Bud6 ₍₄₇₈₋₇₈₈₎	6.8±1.1
	Bud6	Sph1	2.6±0.6
	Sph1	Spa2	3.0±0.6
	Spa2	Sph1	1.3±0.4
	Sph1	Pea2	3.7±0.6
<i>STE5</i>	Sph1†	AD	3.2±0.6
	DBD	Sph1	2.2±0.4
<i>ste5Δ</i>	Sph1	AD	3.2±0.3
	DBD	Sph1	4.8±0.6

*Activity is expressed as nmole of *O*-nitrophenyl- β -D-galactopyranoside hydrolyzed per minute times mg of protein. β -Galactosidase activity was measured from three independent pools of transformants for each set of interactions in either Y864 (*STE5*) or YS85 (*ste5Δ*) as noted. Standard deviations are indicated.

†Interaction was also detected using a Sph1-*GAL4* DNA binding domain fusion plasmid.

SLT2/MPK1 MAP kinase pathway were tested for interaction with Sph1p; Sph1-DBD interacts with Slt2-AD approximately 2- to 3-fold above background (Table 3). However no interaction was observed between Sph1-AD and Slk1-DBD (Table 3).

Since Spa2p associates with both Pea2p and Bud6p (Y.-J. Sheu et al., unpublished observations), additional two-hybrid tests were performed to examine whether Sph1p also interacts with these polarity proteins (Fig. 9C; Table 3). A weak interaction was detected between Sph1-DBD and several Bud6 fragments fused to the Gal4p activation domain, the strongest interaction occurring with a fusion containing the carboxyl-terminal 513 amino acids. Surprisingly, no interaction was observed between Sph1-AD and full length Bud6-DBD. In addition, no significant two-hybrid interactions between Sph1p and full length Pea2- and Spa2-fusion proteins were observed (Fig. 9C; Table 3). Furthermore, no detectable interaction of Sph1p with itself was observed (data not shown).

Sph1p and Spa2p do not affect pseudohyphal signal transduction

Because Spa2p and Sph1p interact with Ste7p and Ste11p by the two-hybrid system, and mutations in these genes result in pseudohyphal defects, we examined whether *SPA2* and/or *SPH1* play any role in the pseudohyphal signal transduction pathway.

Table 4. Expression of *FG(TyA)::lacZ* in haploid and diploid strains

	Relevant genotype	Relative activity	
		SC-Ura	SLAD
Haploids	Wild type	1.0 (93)	1.0 (317)
	<i>spa2Δ</i>	2.3±0.7	1.1±0.1
	<i>sph1Δ</i>	1.4±0.2	0.9±0.2
	<i>spa2Δ sph1Δ</i>	1.4±0.5	0.9±0.1
Diploids	Wild type	1.0 (12)	1.0 (61)
	<i>spa2Δ</i>	0.8±0.3	1.1±0.1
	<i>sph1Δ</i>	1.0±0.2	1.2±0.4
	<i>spa2Δ sph1Δ</i>	1.3±0.3	1.4±0.4

FG(TyA)::lacZ expression was measured in cells growing in nitrogen-rich medium (SC-Ura) or nitrogen-poor medium (SLAD). Activities are expressed as fold difference relative to wild-type β -galactosidase activity. Total β -galactosidase activity of wild type is shown in parentheses and is expressed in nmol of *O*-nitrophenyl- β -D-galactopyranoside hydrolyzed per minute times the mg of protein.

To explore this possibility, β -galactosidase expression was measured from a pseudohyphal and haploid invasive reporter gene (*FG(TyA)-lacZ*) (Mosch et al., 1996) maintained in Σ 1278b wild-type, *spa2Δ*, *sph1Δ*, and *spa2Δ sph1Δ* strains. These strains were grown under nitrogen-rich or nitrogen-poor conditions which promote haploid invasive growth or pseudohyphal growth, respectively. Loss of either *SPH1*, *SPA2*, or both did not appreciably affect the pseudohyphal signaling pathway under the conditions tested (Table 4).

DISCUSSION

SPA2 and the related gene *SPH1* encode a set of proteins important for the control of cell morphogenesis in yeast. *SPA2* and *SPH1* are each required, although to varying extents, for the dimorphic transition between the yeast form and the pseudohyphal cell type. A haploid invasive growth defect as well as a mating projection formation defect in *spa2Δ sph1Δ* cells further support a role for *SPA2* and *SPH1* in polarized growth. Sph1p localizes to sites of polarized growth throughout the budding cycle and during mating projection formation and growth, and Sph1p localization is affected by the loss of *SPA2*. Furthermore, we have demonstrated two-hybrid interactions between Sph1p and several MAP kinase signaling components which parallel interactions between Spa2p and these same kinases (Y.-J. Sheu et al., unpublished observations). These results indicate that Sph1p and Spa2p form a set of proteins that interact with signaling components and mediate polarized cell growth.

SPH1 is a polymorphic gene with homology to *SPA2*

Sequence analysis reveals that *SPH1* is polymorphic, and two distinct strain-specific protein isoforms exist. Liu et al. (1996) have similarly demonstrated a polymorphism in the *FLO8* gene, which in S288C-derived strains blocks haploid invasive and pseudohyphal growth. It is likely the truncated *SPH1* allele contributes to defects in these processes, and may be one of those alleles identified by Lui et al. (1996) that modifies the level of pseudohyphal growth in backcrosses between Σ 1278b

FLO8 and *S288C flo8* strains. Both the *flo8* and *sph1* mutations may have been selected in the process of preparing laboratory strains that form smooth round colonies.

DNA sequence analysis predicts that Sph1p shares several domains of similarity to Spa2p. One such domain contains a pair of direct repeats found at the amino terminus of both proteins. The region containing this domain is important for Spa2p function and is sufficient for interaction with Ste7p, Mkk1p and Mkk2p by two-hybrid analysis (Y.-J. Sheu et al., unpublished observations). Moreover, Arkowitz and Lowe (1997) and Y.-J. Sheu et al. (unpublished observations) have demonstrated that amino-terminal truncations lacking this region of Spa2p, including the first repeat element, results in a mating efficiency comparable to *spa2Δ* cells. Because Sph1p also interacts with Ste7p, Mkk1p, and Mkk2p, we predict that the corresponding amino-terminal domain in Sph1p is likely to be sufficient for this interaction. A GenBank search using this direct repeat sequence identified *H. sapiens* and *C. elegans* genes predicted to encode this SDR motif (Wilson et al., 1994; Nagase et al., 1995), raising the possibility that this domain interacts with MAPK kinases in a wide variety of organisms.

The sequence similarity of Sph1p and Spa2p suggests that other domains shared by the two proteins may also mediate physical associations with additional polarity components. For example, the homologous internal or carboxyl-terminal domains shared between Sph1p and Spa2p are likely to mediate a common interaction between these proteins and other polarity proteins such as Bud6p (Y.-J. Sheu et al., unpublished observations). Conversely, non-homologous domains such as the nine amino acid repeat domain or coiled-coil A region found in Spa2p may mediate distinct physical interactions or specific functions. The presence or absence of specific protein interaction domains is a common feature of cytoskeletal elements that regulate the organization of the actin cytoskeleton. For example, different isoforms of spectrin vary in the presence or absence of protein interaction sites such as those for ankyrin and protein 4.1 (Morrow et al., 1997). Similarly, Sph1p and Spa2p may represent two protein isoforms that interact with and/or modulate the cytoskeleton in different ways.

Sph1p and Spa2p are a partially redundant gene pair

Two significant genetic interactions between the *SPH1* and *SPA2* were identified which indicate that these genes functionally overlap. First, *sph1 spa2* double mutants exhibit a strong haploid invasive growth defect not observed in either *sph1* or *spa2* mutants. Second, *sph1 spa2* double mutants display an exaggerated defect in mating projection morphology as compared to either single mutant. These data, combined with the Sph1p and Spa2p sequence similarity, identical localization profiles in vegetative and mating cells, and overlapping collection of two-hybrid interactions, strongly indicate that *SPH1* and *SPA2* have some functional overlap.

However, contrary to that reported by Arkowitz and Lowe (1997), we were unable to find a bud site selection defect in vegetative *sph1Δ/sph1Δ* cells, despite analyzing three different strains, including the identical strain background used in their study. Moreover, as both studies failed to uncover an exaggerated budding pattern defect in *sph1Δ/sph1Δ*, *spa2Δ/spa2Δ* daughter cells, we believe that *SPH1* does not

functionally overlap with *SPA2* in the process of bud site selection.

The role of Sph1p in polarized cell growth

Localization of Sph1p by immunofluorescence microscopy suggests that Sph1p participates in the process of cellular polarity; the protein localizes to sites of polarized growth in both vegetative and mating cells. Although Sph1p was overexpressed in this study, we believe our results likely reflect the authentic staining pattern for several reasons. First, cells expressing a wide range of Sph1p expression levels all display a similar staining pattern. Second, Arkowitz and Lowe (1997) have reported similar localization results using a GFP-Sph1 fusion protein expressed under the control of a *SPA2* promoter. Third, the observed Sph1p staining pattern is similar to that demonstrated for Spa2p and other polarity proteins during mating and vegetative growth (Snyder, 1989; Pringle et al., 1995). Whether Sph1p is normally expressed in a cell cycle-specific manner is unclear. However, like the *SPA2*, *AXL2*, and *CHS3* polarity genes (Gehring and Snyder, 1990; Roemer et al., 1996a; Santos and Snyder, 1997), *SPH1* contains two predicted MCB elements within its promoter sequence at positions -160 and -167; MCB elements have been shown to activate the expression of several cell cycle-regulated genes at the G₁/S transition (Johnston et al., 1991; Johnston and Lowndes, 1992).

Sph1p may form part of a complex with Spa2p and other polarity proteins. Consistent with this possibility, Sph1p localization is moderately dependent on *SPA2*, perhaps due in part to the partial degradation of Sph1p detected in *spa2Δ* extracts by immunoblot analysis. If Sph1p and Spa2p participate in the formation of a polarity complex, two-hybrid analysis has failed to demonstrate that the two proteins physically associate with one another in this complex. Instead, two-hybrid analyses indicate Sph1p and Spa2p interact in vivo with a common set of polarity and signaling molecules which also associate at sites of active growth.

sph1Δ and *spa2Δ* phenotypes include a wide variety of polarized growth defects including those in haploid invasive growth, pseudohyphal growth, bud site selection, cell shape and mating projection formation. This assortment of phenotypes might be expected if *SPH1* and *SPA2* function in proper organization of the actin cytoskeleton. Mutations in *BNI1*, *PEA2*, *BUD6/AIP3*, and *ACT1* share common diploid budding pattern and pseudohyphal growth phenotypes to the *SPH1-SPA2* gene pair (Mosch and Fink, 1997; Yang et al., 1997). In addition, each of these components localize to sites of polarized growth (Valtz and Herskowitz, 1996; Amberg et al., 1997; Evangelista et al., 1997; Yang et al., 1997). Physical interactions between Bni1p, Bud6p/Aip3p, and Act1p strongly suggest that these components associate indirectly with the actin cytoskeleton (Evangelista et al., 1997). As both Spa2p and Sph1p interact in the two-hybrid system with Bud6p/Aip3p, we speculate that Spa2p and Sph1p may also potentially interact with the actin cytoskeleton.

The *SLT2(MPK1)* MAP kinase pathway is activated during periods of polarized growth and is implicated in maintaining the integrity of the cytoskeleton and cell wall (Igual et al., 1996; Zarzov et al., 1996). A potential target of this pathway is the actin cytoskeleton, since mutations in *SLT2(MPK1)* result in a variety of phenotypes in common with mutants of

the actin cytoskeleton (Costigan et al., 1992; Mazzone et al., 1993; Zarzov et al., 1996). Two-hybrid analysis of both Sph1p and Spa2p (Y.-J. Sheu et al., unpublished observations) demonstrate both of these proteins interact in vivo with the MAPK kinases of the *SLT2(MPK1)* MAP kinase pathway, Mkk1p and Mkk2p. Interestingly, cells containing mutations of both *SPA2* and *SLK1(BCK1)*, which encodes the MAPKKK of this pathway, are lethal (Costigan et al., 1992; Costigan and Snyder, 1994). Furthermore, hyperactivation of this *SLT2(MPK1)* MAP kinase pathway in *spa2* cells, as judged by hyperphosphorylation of Swi6p (a downstream target of Slt2p) (Madden et al., 1997), demonstrates that *SPA2* is physiologically relevant to the activity of this pathway (Y.-J. Sheu et al., unpublished observations). These data indicate that a functional relationship likely exists between Spa2p, Sph1p, and the *SLT2* MAP kinase pathway.

Why have so many proteins that participate in polarized cell growth? There are two possibilities. First, although *spa2*, *sph1*, *pea2*, *bud6*, *bem1*, and *bni1* mutants possess clear polarity defects, these components are not essential for polarized growth (Gehring and Snyder, 1990; Chenevert et al., 1992; Valtz and Herskowitz, 1996; Amberg et al., 1997; Evangelista et al., 1997). Thus, it is possible that they carry out redundant functions in controlling actin polarization in yeast. Consistent with this possibility *spa2Δ bem1Δ* double mutants are dead (Costigan et al., 1992). Second, perhaps these different proteins link the actin cytoskeleton to the cortex in different ways or respond to extracellular signals differently to help specify cell shape. This would be particularly critical during mating projection formation and orientation, which involves the dynamic reorganization of the cytoskeleton while tracking pheromone gradients. Loss of any of these proteins results in defects in mating projection formation.

The role of Sph1p and Spa2p in pseudohyphal growth and haploid invasive growth

Sph1p and Spa2p are important for pseudohyphal growth and haploid invasive growth. This is likely to be due in part to the fact that *spa2Δ sph1Δ* cells remain round and do not elongate, and perhaps to their budding pattern defect.

Surprisingly, examination of the wild-type budding pattern in a population of pseudohyphal cells revealed a bipolar budding program in which most cells possess bud scars at both poles, similar to vegetative cells. This observation is different from the unipolar budding pattern previously described (Kron et al., 1994). This difference, in part, might reflect the fact that Kron et al. concentrated their analysis on cells at the periphery of the colony or on cells that had been freshly transferred to nitrogen-limiting medium; this might bias towards mother cells that bud at the same pole. Our study analyzed all cells in an invasive colony as well as on its surface. Regardless, both our studies and the Kron et al. studies indicate that pseudohyphal daughter cells bud from the distal tip. This feature, in combination with: (1) invasive growth deep into the agar which restricts movement between cells, (2) a cytokinesis defect which enables cells to remain attached, and (3) an elongated cell shape restricting bud formation to the extreme tip of the cell, all likely contributes to the extensive filaments formed by pseudohyphal cells.

Two-hybrid studies using both Sph1p and Spa2p suggest that each of these proteins interact strongly in vivo with the Ste11p

and Ste7p components, but not with Fus3p (Y.-J. Sheu et al., unpublished observations). Like *SPA2* and *SPH1*, both *STE7* and *STE11* are required for haploid invasive growth and pseudohyphal defects; *FUS3* is not. Thus, Spa2p and Sph1p may affect pseudohyphal and haploid invasive growth through interaction with these signaling components. Deletion of *SPA2* and *SPH1* did not significantly affect the activity of a pseudohyphal and haploid invasive reporter construct, indicating that overall signaling is not impaired in these strains. Moreover, Y.-J. Sheu et al. (unpublished observations) demonstrate that a mating reporter construct is only slightly affected by the presence of a low level of pheromone.

There are two possibilities as to how Sph1p and Spa2p interactions with Ste11p and Ste7p might affect signaling. First, the localization of Sph1p and Spa2p resembles the localization pattern of Ste20p; perhaps Ste7p and Ste11p are polarized as well. Spa2p and Sph1p might help localize these components at growth sites and affect signaling specifically at these locations. A second possibility, not mutually exclusive from the first, is that Sph1p and Spa2p might serve as a scaffold for mediating interactions among signaling components of MAP kinase cascades. Ste5p has been shown to interact directly with many elements in the pheromone-response MAP kinase module and serves as the archetype for a 'scaffolding' protein. Such molecules are able to link multiple components in a kinase cascade to one another, thereby amplifying the output signal of the kinase cascade and restricting undesirable crosstalk between MAP kinase cascades (Choi et al., 1994; Yashar et al., 1995). One intriguing possibility is that Sph1p and Spa2p function in an analogous manner to Ste5p during haploid invasive and pseudohyphal growth. Because interactions between Sph1p and Spa2p (Y.-J. Sheu et al., unpublished observations) with Ste7p and Ste11p occur independently of Ste5p, and because *STE5* does not appear to participate in either the haploid invasive or pseudohyphal morphogenic pathways (and in fact is not expressed in diploid cells; Leberer et al., 1993), Sph1p and Spa2p may functionally replace Ste5p in tethering the Ste11p-Ste7p signaling module to sites of polarized growth during periods of environmental stress.

A growing number of structurally unrelated proteins in yeast and other eukaryotic cells are now believed to function as molecular scaffolds. In yeast, the MAPKK Pbs2p, has recently been demonstrated to interact with each of the constituent components of the HOG high osmolarity signal pathway, and is proposed to restrict osmotic stress-activated Ste11p to phosphorylating only Pbs2p (Posas and Saito, 1997). Similarly in mammalian cells, a class of A kinase anchoring proteins known as AKAPs, have been reported (Coghlan et al., 1995). AKAP79 and AKAP250 interact with protein kinase A, protein kinase C, and calcineurin signaling molecules and each of these proteins share a similar subcellular distribution in neurons (Klauck et al., 1996; Nauert et al., 1996). Since at least five distinct MAP kinase modules exist in yeast (Herskowitz, 1995; Waskiewicz and Cooper, 1995), each of which may be differentially localized and/or regulated under different conditions, novel scaffolding proteins are likely to be uncovered. Future studies will determine whether Sph1p and Spa2p directly interact with Ste11p or Ste7p, and whether these interactions occur simultaneously as predicted for a multivalent protein scaffold.

We thank Charlie Boone, Elaine Elion, Gerald Fink, Ekkehard Leberer, and George Sprague for kindly providing plasmids. We also thank Jennifer Barrett, Beatriz Santos, and Susana Vidan for critical comments on the manuscript, and Yi-Lun Liu for assistance in pseudohyphal growth studies. We thank Jeff Segall and Michael Cammer for allowing us to utilize the Einstein Analytical Imaging Facility to produce Fig. 4. T.R. was supported by a Medical Research Council of Canada postdoctoral fellowship. This research was supported by National Institutes of Health grant GM36494.

REFERENCES

- Amberg, D. C., Zahner, J. E., Mulholland, J. W., Pringle, J. R. and Botstein, D. (1997). Aip3p/Bud6p, a yeast actin-interacting protein that is involved in morphogenesis and the selection of bipolar budding sites. *Mol. Cell Biol.* **17**, 729-753.
- Arkowitz, R. A. and Lowe, N. (1997). A small conserved domain in the yeast Spa2p is necessary and sufficient for its polarized localization. *J. Cell Biol.* **138**, 17-36.
- Baudin, A., Ozier-Kalogeropoulos, O., Denouel, A., Lacroute, F. and Cullin, C. (1993). A simple and efficient method for direct gene deletion in *Saccharomyces cerevisiae*. *Nucl. Acids Res.* **21**, 3329-3330.
- Bender, A. and Pringle, J. R. (1989). Multicopy suppression of the *cdc24* budding defect in yeast by *CDC42* and three newly identified genes including the *ras*-related gene *RSR1*. *Proc. Nat. Acad. Sci. USA* **86**, 9976-9980.
- Blacketer, M. J., Koehler, C. M., Coats, S. G., Myers, A. M. and Madaule, P. (1993). Regulation of dimorphism in *Saccharomyces cerevisiae*: involvement of the novel protein kinase homolog Elm1p and protein phosphatase 2A. *Mol. Cell Biol.* **13**, 5567-5581.
- Blacketer, M. J., Madaule, P. and Myers, A. M. (1994). The *Saccharomyces cerevisiae elm4-1* facilitates pseudohyphal differentiation and interacts with a deficiency in phosphoribosylpyrophosphate synthase activity to cause constitutive pseudohyphal growth. *Mol. Cell Biol.* **14**, 4671-4681.
- Burns, N., Grimwade, B., Ross-Macdonald, P. B., Choi, E.-Y., Finberg, K., Roeder, G. S. and Snyder, M. (1994). Large-scale characterization of gene expression, protein localization and gene disruption in *Saccharomyces cerevisiae*. *Genes Dev.* **8**, 1087-1105.
- Chant, J. and Herskowitz, I. (1991). Genetic control of bud-site selection in yeast by a set of gene products that comprise a morphogenetic pathway. *Cell* **65**, 1203-1212.
- Chant, J. and Pringle, J. R. (1995). Patterns of bud site selection in the yeast *Saccharomyces cerevisiae*. *J. Cell Biol.* **129**, 751-765.
- Chenevert, J., Corrado, K., Bender, A., Pringle, J. and Herskowitz, I. (1992). A yeast gene (*BEMI*) necessary for cell polarization whose product contains two SH3 domains. *Nature* **356**, 77-79.
- Chenevert, J., Valtz, N. and Herskowitz, I. (1994). Identification of genes required for normal pheromone-induced cell polarization in *Saccharomyces cerevisiae*. *Genetics* **136**, 1287-1297.
- Choi, K.-Y., Satterberg, B., Lyons, D. M. and Elion, E. A. (1994). Ste5 tethers multiple protein kinases in the MAP kinase cascade required for mating in *S. cerevisiae*. *Cell* **78**, 499-512.
- Coghlan, V. M., Perrino, B. A., Howard, M., Langeberg, L. K., Hicks, J. B., Gallatin, W. M. and Scott, J. D. (1995). Association of protein kinase A and protein phosphatase 2B with a common anchoring protein. *Science* **267**, 108-111.
- Costigan, C., Gehrung, S. and Snyder, M. (1992). A synthetic lethal screen identifies SLK1, a novel protein kinase homolog implicated in yeast cell morphogenesis and cell growth. *Mol. Cell Biol.* **12**, 1162-1178.
- Costigan, C. and Snyder, M. (1994). SLK1, a homolog of MAP kinase activators, mediates nutrient sensing independently of the yeast cAMP-dependent protein kinase pathway. *Mol. Gen. Genet.* **243**, 286-296.
- Costigan, C., Kolodrubetz, D. and Snyder, M. (1994). NHP6A and NHP6B, which encode HMG1-like proteins, are candidates for downstream components of the yeast SLT2 mitogen-activated protein kinase pathway. *Mol. Cell Biol.* **14**, 2391-2403.
- Drubin, D. G. and Nelson, W. J. (1996). Origins of cell polarity. *Cell* **84**, 335-344.
- Evangelista, M., Blundell, K., Longtine, M. S., Chow, C. J., Adames, N., Pringle, J. R., Peter, M. and Boone, C. (1997). Bni1p, a yeast formin linking Cdc42p and the actin cytoskeleton during polarized morphogenesis. *Science* **276**, 118-122.
- Fields, S. and Song, O.-K. (1989). A novel genetic system to detect protein-protein interactions. *Nature* **340**, 245-246.
- Flescher, E. G., Madden, K. and Snyder, M. (1993). Components required for cytokinesis are important for bud site selection in yeast. *J. Cell Biol.* **122**, 373-386.
- Foreman, P. K. and Davis, R. W. (1994). Cloning vectors for the synthesis of epitope tagged, truncated and chimeric proteins in *Saccharomyces cerevisiae*. *Gene* **144**, 63-68.
- Freifelder, D. (1960). Bud position in *Saccharomyces cerevisiae*. *J. Bacteriol.* **124**, 511-523.
- Gavrias, V., Andrianopoulos, A., Gimeno, C. J. and Timberlake, W. E. (1996). *Saccharomyces cerevisiae TEC1* is required for pseudohyphal growth. *Mol. Microbiol.* **19**, 1255-1263.
- Gehrung, S. and Snyder, M. (1990). The *SPA2* gene of *Saccharomyces cerevisiae* is important for pheromone-induced morphogenesis and efficient mating. *J. Cell Biol.* **111**, 1451-1464.
- Gimeno, C. J., Ljungdahl, P. O., Styles, C. A. and Fink, G. R. (1992). Unipolar cell divisions in the yeast *S. cerevisiae* lead to filamentous growth: regulation by starvation and *RAS*. *Cell* **68**, 1077-1090.
- Gimeno, C. J. and Fink, G. R. (1994). Induction of pseudohyphal growth by overexpression of *PHD1*, a *Saccharomyces cerevisiae* gene related to transcriptional regulators of fungal development. *Mol. Cell Biol.* **14**, 2100-2112.
- Guthrie, C. and Fink, G. R. (1991). Guide to yeast genetics and molecular biology. *Meth. Enzymol.* **194**.
- Herskowitz, I. (1995). MAP kinase pathways in yeast: for mating and more. *Cell* **80**, 187-197.
- Igual, J. C., Johnson, A. L. and Johnston, L. H. (1996). Coordinated regulation of gene expression by the cell cycle transcription factor Swi4 and the protein kinase C MAP kinase pathway for yeast cell integrity. *EMBO J.* **15**, 5001-5013.
- Johnston, L. H., Lowndes, N. F., Johnson, A. L. and Sugino, A. (1991). A cell-cycle-regulated trans-factor, DSC1, controls expression of DNA synthesis genes in yeast. *Cold Spring Harbor Symp. Quant. Biol.* **56**, 169-176.
- Johnston, L. H. and Lowndes, N. F. (1992). Cell cycle control of DNA synthesis in budding yeast. *Nucl. Acids Res.* **20**, 2403-2410.
- Johnston, M., Hillier, L., Riles, L., Albermann, K., Andre, B., Ansoorge, W., Benes, C., Bruckner, M., Delius, H., Dubois, E. et al. (1997). The nucleotide sequence of *Saccharomyces cerevisiae* chromosome XII. *Nature* **387**, 87-90.
- Klauck, T. M., Faux, M. C., Labudda, K., Langeberg, L. K., Jaken, S. and Scott, J. D. (1996). Coordination of three signaling enzymes by AKAP79, a mammalian scaffold protein. *Science* **271**, 1589-1592.
- Kron, S. J., Styles, C. A. and Fink, G. R. (1994). Symmetric cell division in pseudohyphae of the yeast *Saccharomyces cerevisiae*. *Mol. Biol. Cell.* **5**, 1003-1022.
- Laemmli, U. K. (1970). Cleavage of structural proteins during the assembly of the head of bacteriophage T4. *Nature* **227**, 680-685.
- Leberer, E., Dignard, D., Hargus, D., Hogan, L., Whiteway, M. and Thomas, D. Y. (1993). Cloning of *Saccharomyces cerevisiae STE5* as a suppressor of a Ste20 protein kinase mutant: structural and functional similarity of Ste5 to Far1. *Mol. Gen. Genet.* **241**, 241-254.
- Leberer, E., Wu, C., Leeuw, T., Fourest-Lieuvin, A., Segall, J. E. and Thomas, D. Y. (1997). Functional characterization of the Cdc42p binding domain of yeast Ste20p protein kinase. *EMBO J.* **16**, 83-97.
- Lew, D. and Reed, S. (1995). Cell cycle control of morphogenesis in budding yeast. *Curr. Opin. Genet. Dev.* **5**, 17-23.
- Liu, H., Styles, C. A. and Fink, G. R. (1993). Elements of the yeast pheromone response pathway required for filamentous growth of diploids. *Science* **262**, 1741-1744.
- Lui, H., Krizek, J. and Bretcher, A. (1993). Construction of a *GAL1*-regulated yeast cDNA expression library and its application to the identification of genes whose overexpression causes lethality in yeast. *Genetics* **132**, 665-673.
- Liu, H., Styles, C. A. and Fink, G. R. (1996). *Saccharomyces cerevisiae* S288C has a mutation in *FLO8*, a gene required for filamentous growth. *Genetics* **144**, 967-978.
- Madden, K., Sheu, Y.-J., Baetz, K., Andrews, B. and Snyder, M. (1997). SBF cell cycle regulator as a target of the yeast SLT2 MAP kinase pathway. *Science* **275**, 1781-1784.
- Madden, K. and Snyder, M. (1992). Specification of sites of polarized growth

- in *Saccharomyces cerevisiae* and the influence of external factors on site selection. *Mol. Biol. Cell* **3**, 1025-1035.
- Madhani, H. D. and Fink, G. R.** (1997). Combinatorial control required for the specificity of yeast MAPK signaling. *Science* **275**, 1314-1317.
- Mazzoni, C., Zarzov, P., Rambourg, A. and Mann, C.** (1993). *SLT2(MPK1)* MAP kinase homolog is involved in polarized cell growth in *Saccharomyces cerevisiae*. *J. Cell Biol.* **123**, 1821-1823.
- Morrow, J. S., Rimm, D. L., Kennedy, S. P., Cianci, C. D., Sinard, J. H. and Weed, S. A.** (1997). Of membrane stability and mosaics: the spectrin cytoskeleton. In *Handbook of Physiology* (ed. J. Hoffman and J. Jamieson), pp. 485-540. Oxford University Press, London.
- Mosch, H., Roberts, R. and Fink, G.** (1996). Ras2 signals via the Cdc42/Ste20/mitogen-activated kinase module to induce filamentous growth in *Saccharomyces cerevisiae*. *Proc. Nat. Acad. Sci. USA* **93**, 5352-5356.
- Mosch, H.-U. and Fink, G. R.** (1997). Dissection of filamentous growth by transposon mutagenesis in *Saccharomyces cerevisiae*. *Genetics* **145**, 671-684.
- Nagase, T., Seki, N., Tanaka, A., Ishikawa, K. and Nomura, N.** (1995). Prediction of the coding sequence of unidentified human genes. IV. The coding sequence of 40 new genes (KIAA0121-KIAA0160) deduced by analysis of cDNA clones from human cell line KG-1. *DNA Res.* **2**, 167-174.
- Nauert, J. B., Klauck, T. M., Langeberg, L. K. and Scott, J. D.** (1996). Gravin, an autoantigen recognized by serum from myasthenia gravis patients, is a kinase scaffold protein. *Curr. Biol.* **7**, 52-62.
- Posas, F. and Saito, H.** (1997). Osmotic activation of the HOG MAPK pathway via Ste11p MAPKKK: scaffold role of Pbs2p MAPKK. *Science* **276**, 1702-1705.
- Pringle, J., Bi, E., Harkins, H., Zahner, J., Devirgilio, C., Chant, J., Corado, K. and Fares, H.** (1995). Establishment of cell polarity in yeast. *Cold Spring Harbor Symp. Quant. Biol.* **60**, 729-744.
- Printen, J. A. and Sprague, G. F. Jr** (1994). Protein-protein interactions in the yeast pheromone response pathway: Ste5p interacts with all members of the MAP kinase cascade. *Genetics* **138**, 609-619.
- Roberts, R. and Fink, G. R.** (1994). Elements of a single MAP kinase cascade in *Saccharomyces cerevisiae* mediate two developmental programs in the same cell type: mating and invasive growth. *Genes Dev.* **8**, 2974-2985.
- Roemer, T., Madden, K., Chang, J. and Snyder, M.** (1996a). Selection of axial growth sites in yeast requires Axl2p, a novel plasma membrane glycoprotein. *Genes Dev.* **10**, 777-793.
- Roemer, T., Vallier, L. G. and Snyder, M.** (1996b). Selection of polarized growth sites in yeast. *Trends Cell Biol.* **6**, 434-441.
- Sambrook, J., Fritsch, E. F. and Maniatis, T.** (1989). *Molecular Cloning: A Laboratory Manual*. Cold Spring Harbor Laboratory Press, Cold Spring Harbor, New York.
- Santos, B. and Snyder, M.** (1997). Targeting of chitin synthase 2 to polarized growth sites in yeast requires Chs5p and Myo2p. *J. Cell Biol.* **136**, 95-110.
- Schneider, B. L., Seufert, W., Steiner, B., Yang, Q. H. and Futcher, A. B.** (1995). Use of PCR epitope tagging for protein tagging in *Saccharomyces cerevisiae*. *Nucl. Acids Res.* **11**, 1265-1274.
- Sikorski, R. and Hieter, P.** (1989). A system of shuttle vectors and yeast host strains designed for efficient manipulation of DNA in *Saccharomyces cerevisiae*. *Genetics* **122**, 19-27.
- Snyder, M.** (1989). The SPA2 protein of yeast localizes to sites of cell growth. *J. Cell Biol.* **108**, 1419-1429.
- Snyder, M., Gehrung, S. and Page, B. D.** (1991). Studies concerning the temporal and genetic control of cell polarity in *Saccharomyces cerevisiae*. *J. Cell Biol.* **114**, 515-532.
- Sprague, G. F. and Thorner, J.** (1992). Pheromone response and signal transduction during the mating process of *Saccharomyces cerevisiae*. In *The Molecular Biology of the Yeast Saccharomyces* (ed. J. R. Broach, J. R. Pringle and E. W. Jones), pp. 657-744. Cold Spring Harbor Laboratory Press, Cold Spring Harbor, New York.
- Steinert, P. M. and Roop, R.** (1988). The molecular and cellular biology of intermediate filaments. *Annu. Rev. Biochem.* **57**, 593-625.
- Traverse, S., Gomez, N., Paterson, H., Marshall, C. and Cohen, P.** (1992). Sustained activation of the mitogen-activated protein (MAP) kinase cascade may be required for differentiation of PC12 cells. Comparison of the effects of nerve growth factor and epidermal growth factor. *Biochem. J.* **288**, 351-355.
- Valtz, N. and Herskowitz, I.** (1996). Pea2 protein of yeast is localized to sites of polarized growth and is required for efficient mating and bipolar budding. *J. Cell Biol.* **135**, 725-739.
- Waskiewicz, A. and Cooper, J. A.** (1995). Mitogen and stress response pathways: MAP kinase cascades and phosphatase regulation in mammals and yeast. *Curr. Opin. Cell Biol.* **7**, 798-805.
- Wilson, R., Ainscough, R., Anderson, K., Baynes, C., Berks, M., Bonfield, J., Burton, J., Connell, M., Copsey, T. and Cooper, J. et al.** (1994). 2.2 Mb of contiguous nucleotide sequence from chromosome III of *C. elegans*. *Nature* **368**, 32-38.
- Xie, K., Lambie, E. and Snyder, M.** (1993). Nuclear dot antigens may specify transcriptional domains in the nucleus. *Mol. Cell. Biol.* **13**, 6170-6179.
- Yang, S., Ayscough, K. R. and Drubin, D. G.** (1997). A role for the actin cytoskeleton of *Saccharomyces cerevisiae* in bipolar bud-site selection. *J. Cell Biol.* **136**, 111-123.
- Yashar, B., Ire, K., Printen, J. A., Stevenson, B. J., Sprague, G. F. Jr, Matsumoto, K. and Errede, B.** (1995). Yeast MEK-dependent signal transduction: response thresholds and parameters affecting fidelity. *Mol. Cell. Biol.* **15**, 6545-6553.
- Yorihuzi, T. and Ohsumi, Y.** (1994). *Saccharomyces cerevisiae* *MATa* mutant cells defective in pointed projection formation in response to α -factor at high concentrations. *Yeast* **10**, 579-594.
- Zahner, J. E., Harkins, H. A. and Pringle, J. R.** (1996). Genetic analysis of the bipolar pattern of bud site selection in the yeast *Saccharomyces cerevisiae*. *Mol. Cell. Biol.* **16**, 1857-1870.
- Zarzov, P., Mazzoni, C. and Mann, C.** (1996). The SLT2 (MPK1) MAP kinase is activated during periods of polarized cell growth in yeast. *J. EMBO* **15**, 83-91.
- Zervos, A. S., Gyuris, J. and Brent, R.** (1993). Mxi, a protein that specifically interacts with Max to bind Myc-Max recognition sites. *Cell* **72**, 223-232.